EXPERIMENT DESIGN IN COMPLIANT MECHANISMS AND KINEMATIC IDENTIFICATION OF PARALLEL MECHANISMS

EXPERIMENT DESIGN IN COMPLIANT MECHANISMS AND KINEMATIC IDENTIFICATION OF PARALLEL MECHANISMS

David Restrepo Arango

EAFIT UNIVERISTY
SCHOOL OF ENGINEERING
MECHANICAL ENGINEERING DEPARTMENT
MEDELLIN
2010

EXPERIMENT DESIGN IN COMPLIANT MECHANISMS AND KINEMATIC IDENTIFICATION OF PARALLEL MECHANISMS

David Restrepo Arango

Graduation project submitted to the Department of Mechanical Engineering in partial fulfillment of the requirements for the degree of Bachelor of Science in Mechanical Engineering at the EAFIT University

April 2010

Advisor
Prof. Dr. Eng Oscar E. Ruiz

EAFIT UNIVERISTY
SCHOOL OF ENGINEERING
MECHANICAL ENGINEERING DEPARTMENT
MEDELLIN
2010

ACKNOWLEDGMENTS

To my family that set on me the responsibility and example of hard work, and for all their love and encouragement specially in hardest moments.

My sincere gratitude to my advisor, Prof.Dr.Eng. Oscar Ruiz, for his reliable support, his guidance and invaluable supervision during this work. Many thanks to Prof.Dr.Eng. Diego A. Acosta for his advice and help with the technical revision of some parts of this work.

Deep thanks to my friends and colleagues at the CAD CAM CAE Laboratory at EAFIT University, specially Sebastian Durango and Jorge Correa that have been source of joy, support and technical help.

Many thanks to my friends and classmates in Mechanical Engineering at EAFIT. I have had a very happy time with them during these years.

Also I wish to acknowledge the financial support for this research via the Colombian Administrative Department of Sciences, Technology and Innovation (COLCIENCIAS grant 479 - 2008), EAFIT University (COL) and Autonoma de Manizales University (COL).

CONTENTS

LIST OF FIGURES

LIST OF TABLES

1 INTRODUCTION

Mechanisms are mechanical devices that are used to transfer motion, force or energy in a mechanical system [2]. The kinematic analysis of mechanisms refers to the study of the motion of the mechanism while it is being operated. This consist principally on a set of techniques used to determine the positions, velocities and accelerations of certain points on the members of the mechanisms.

The general problem of kinematic analysis in mechanisms, has an important subproblem in the assessment of the sources causing errors of relative position and orientation (pose) between an intended output path and the actually achieved path of an end-effector. Such relative pose errors are caused by: (1) fabrication tolerances and assembly errors of the machine elements, (2) weight of the links, (3) deformation of the members of the mechanism, (4) inertial and workload forces and thermal or other sources [3].

Relative position errors varying slowly in time are related to the structure of the machine itself. Therefore, they can be modeled as geometric parameters associated with the structure of the machine [4]. The process of estimation of geometric parameters in mechanisms and manipulators is called *kinematic identification* [5]. With accurate kinematic identification it is possible to minimize the relative position errors in mechanism improving its accuracy [6].

In some cases deformations of the members that constitute a mechanism are desired. This type of mechanisms are known as *compliant mechanisms*. Compliant mechanisms (CMs) are an instance of mechanical devices designed to transfer or transmit motion, force, or energy from specified input ports to output ports by elastic deformation of at least one of its members. In these mechanisms the deformations are the goal to achieve, and not a behavior to minimize.

Kinematic identification of mechanism, and modeling and analysis of compliant mechanisms are open research fields for its importance in technical developments in which high accuracy and precision of mechanical devices is required (*e.g.* nanotechnology, medical devices, high performance manufacturing machines, etc.).

This document presents two strategies developed for the prediction of quasi-static

deformations in mechanisms. In chapter 2 Intentional deformations in compliant mechanisms are addressed. On this chapter it is proposed a new methodology to force-displacement model of compliant mechanisms under quasi-static conditions by computer design of experiments. Non-intentional deformations are studied in chapter 3. On this chapter a new protocol for kinematic identification of parallel mechanisms is developed. Chapter 4 presents the general conclusions of the work presented on this document.

The work presented on this document is part of the research project **GEOMETRIC ERROR MODELING IN MECHANISMS**. The strategies presented have been devised and implemented in the CAD CAM CAE Laboratory at EAFIT University under the supervision of Prof.Dr.Eng. Oscar E. Ruiz.

2 DESIGN OF COMPUTER EXPERIMENTS APPLIED TO MODELING COMPLIANT MECHANISMS

2.1 CONTEXT

Since 2007 the CAD CAM CAE Laboratory at EAFIT University, started the research project **GEOMETRIC ERROR MODELING IN MECHANISMS**. The goal of the project is to predict quasi-static deformations of mechanisms. Two types of deformations are considered: (1) Non-intentional and (2) Intentional. In traditional (kinematic joint-based) mechanisms the deformation is non-intentional and it is in general considered as negative. In contrast, there are mechanisms in which the deformation is intentional. In these mechanisms (called compliant) the functioning is precisely allowed by the deformation, since there are no kinematic joints (prismatic, revolute, spheric, etc.).

This chapter concentrates on the prediction of deformations in compliant mechanisms, presenting a new force-displacement modeling method based on computer Design of Experiments (DOE). The force-displacement modeling is proposed to be developed by a systematic Design of computer Experiments that is aimed to find the main input factors (*e.g.* input loads) and its interactions and to fit a mathematical model that represents the input-output (force-displacement) behavior.

With respect to traditional force-position modeling of compliant mechanisms our proposal has the goals: (1) To developed a force-displacement modeling methodology general enough to cover both lumped and fully compliant mechanisms. (2) To obtain input-output models simple enough to be used in real-time control. (3) To replace physical experimentation by computer simulations reducing costs in product development.

The content of this chapter corresponds to the article "Design Of Computer Experiments Applied To Modeling Of Compliant Mechanisms" by David Restrepo, Diego Acosta, Sebastian Durango, Oscar Ruiz, accepted for publication in the Eighth In-

ternational Symposium on Tools and Methods of Competitive Engineering. April 12 - 16, 2010, Ancona, Italy.

As co-authors of such publication, we give our permission for this material to appear in this document. We are ready to provide any additional information on the subject, as needed.

Prof. Dr. Eng. Oscar E. Ruiz
oruiz@eafit.edu.co
Coordinator CAD CAM CAE Laboratory
EAFIT University, Medellin, COLOMBIA

Prof. Dr. Eng. Diego A. Acosta
dacostam@eafit.edu.co
DDP Research Group
EAFIT University, Medellin, COLOMBIA

M.Sc. Sebastian Durango
sdurang1@eafit.edu.co
PhD student at CAD CAM CAE Laboratory
EAFIT University, Medellin, COLOMBIA

2.2 Abstract

This article discusses a procedure for force-displacement modeling compliant mechanisms by using a design of computer experiments methodology. This approach produces a force-displacement meta-model that is suited for real-time control of compliant mechanisms. The term meta-model is used to represent a simplified and efficient mathematical model of unknown phenomena. The meta-modeling of compliant mechanisms is performed from virtual experiments based on factorial- and space-filling design of experiments. The procedure is used to model the quasi-static behavior of the HexFlex compliant mechanism. The HexFlex is a parallel compliant mechanism for nano-manipulation that allows six degrees of freedom of its moving stage. The meta-model of the HexFlex is calculated from experiments with the Finite Element Method (FEM).The obtained meta-model for the HexFlex is linear for the range of movement of the mechanism. The accuracy of the meta-model was calculated conducting a set of computer experiments with random uniform distribution of the input forces. Three criteria were calculated in each displacement direction $(x, y, z, \theta_x, \theta_y, \theta_z)$ comparing the meta-model prediction with respect to the results of the virtual experiments: 1. maximum of the absolute value of the error, 2. relative error, and 3. root mean square error. The maximum errors were founded adequate with respect to demanding manufacturing tolerances (absolute errors) and lower than errors reported by other authors (relative errors).

Nomenclature

XYZ	–	Fixed reference coordinate system
T1	–	Input force port on Tab1
T2	–	Input force port on Tab2
T3	–	Input force port on Tab3
D1	–	Direction parallel to the connection beams in the HexFlex
D2	–	Direction perpendicular to the plane that contains the HexFlex on its relaxed position
τ	–	Vector of input forces and torques
$\mathbf{r}$	–	Vector with the end-effector pose
x,y,z	–	Coordinates of a point in XYZ frame
θ_x, θ_y, θ_z	–	Set of Euler angles of a rigid body

2.3 Introduction

Compliant mechanisms (CMs) are an instance of mechanical devices designed to transfer or transmit motion, force, or energy from specified input ports to output ports by elastic deformation of at least one of its members. The main advantage of compliant mechanisms with respect to traditional rigid-link mechanism is that fewer parts, fewer assembly process and no lubrication are required [7]. Due to the complexity of their motion, compliant mechanisms are difficult to design and analyze by traditional kinematic methods [8].

Force-displacement modeling of CMs is required to accurately design a model-based control. Three main methods ([9]) are available for the modeling and design of CMs: (1) the Pseudo Rigid Body Model (PRBM), (2) topology optimization and (3) numerical methods. The PRBM considers a compliant mechanism as being a traditional static structure where the joints are produced by concentrated elasticity zones ([10, 11, 12]) which concentrate the flexibility (lumped compliance). For topology optimization a performance function is proposed, which achieves different values for each alternative of the topology or geometry of the structure. Achieving "good" values of the performance functions closely relates to a "desirable" structure (both in geometrical and topological terms) [13, 14, 15]. This approach reduces human intervention in the design but gives as a result structures that can be impossible to build [16]. Strategies based on numerical methods are time consuming both in the modeling and in the computation [11] being useful for design tasks but not for real-time motion control. The lack of tools to model CMs is recognized as an open research problem [11].

This article presents a methodology for Force (Input) - Displacement (Output) modeling of compliant mechanisms under quasi-static conditions using computer experiments. The methodology allows to find an approximate mathematical model (meta-modeling) of the mechanism that has direct application in controlling it in real time. Finite Element Analysis is used to find and fit the meta-model, but not in the time of the mechanism operation. This modeling is suitable for mechanisms with lumped or distributed compliance. The term *meta-model* in computer experiments represents a surrogate model based on the use of statistical techniques to yield mathematical equations that approximate the results rendered by computer algorithms such as

Finite Elements Analysis [17]. If the true nature of a computer analysis code is

$$u = w(\mathbf{v})$$

where $\mathbf{v}$ are the inputs and u are the outputs of the computer code; then a surrogate model or *meta-model* of the analysis code is

$$\widehat{u} = z(\mathbf{v})$$

where $\widehat{u}$ is is an approximation of the outputs of the computer code

$$\widehat{u} = u + \epsilon$$

where ϵ is the approximation error.

Meta-models have benefits in screening variables, reducing design costs and optimizing design ([18]). They are applied here to model the quasi-static behavior of the HexFlex mechanism. The HexFlex is a six degrees of freedom parallel compliant mechanism with distributed compliance for nano-manipulating designed in MIT by Martin L. Culpepper and Gordon Anderson [19, 20].

The layout of this article is as follows. Section 2.4 presents the literature and contributions reviewed. Section 2.5 presents the proposed methodology, and its scope, for force-displacement modeling of CMs under quasi-static conditions. The case study "HexFlex" Compliant Mechanism is presented in section 2.6. Section 2.7 concludes the article.

2.4 Literature review. Modeling of compliant mechanisms

Three main methods of analysis and design of compliant mechanisms (CMs) are considered [9]: the pseudo rigid body model (PRBM), the topology optimization and numerical methods. The fundamentals of these methods are summarized in the following literature review.

2.4.1 Pseudo Rigid Body Modeling (PRBM)

PRBM is used to design *static structures* which behave as *movable mechanisms*. In the structure, local regions (*e.g.* flexural joints, notch hinges) are chosen which are intentionally weakened and therefore undergo large deformations having what is called *lumped compliance*. In this manner, the structure behaves as a mechanism (i.e. has degrees of freedom) although strictly speaking no kinematic joints are present.

In the designed structure the PRBM distinguishes between strong and weak components. The first are modeled as completely rigid. The later produce the mobility of the mechanism. They are displacement and torsional springs, non-linear elastic beams, etc. These hyper-flexible members can be analyzed with closed differential equations (e.g. flexural cantilever beam). In the PRBM model the stiff members do not deform, and therefore the deformed ones absorb the whole angular displacement, therefore becoming a *rotational* joint.

A key step of the PRBM is to estimate the equivalent application point and equivalent elastic constant of the spring represented by the flexible cantilever beam.

The PRBM approach is mathematically addressed under two theories to solve the strains formulation: 1. Linear formulation. 2. Non-linear formulation. This basically means that the mathematical distinction between the linear and nonlinear formulation lies in the way in which the strains are expressed in terms of displacements.

From theory of elasticity it is well known that strains can be formulated as functions of the partial derivatives of the displacement functions, and that higher-order partial derivatives are usually involved. The linear formulation neglect partial derivatives that have an order or power grater than one. The following articles present linear PRBM as part of their formulation: In [21] an analytical scheme for the displacement analysis of micro-positioning stages with flexural hinges is presented. The scheme replaces the hinges by linear springs, allowing to create simple input/output models of the mechanisms based on their elastic energy equations. Analytical models of revolute and translational compliant joints are presented in [22]. In [23] PRBM is applied in predicting the behavior of a nano - scale parallel guiding mechanism which uses two carbon nano - tubes as flexural links. The kinematic behavior accuracy

reported was within 7,3% of error with respect to a molecular simulation. Reference [24] presents the design of a three degree of freedom compliant planar mechanisms based on the 3RRR rigid mechanism. The design of bistable compliant mechanisms based on the PRBM and calculations of the potential energy and moment required to move it to a particular position is presented in [25]. In reference [26] the kinematic and force analysis of compliant driven robotic mechanisms is made based on equations that relate joint torques, joint angles and displacements. The input / output model of a 3RRR compliant micro-motion stage replacing its flexures with a set of equivalent springs is presented in [27].

Non-linear PRBM is based principally on the application of Euler beam models or deflection models based on the Castigliano‘s second theorem to model the flexible members of the compliant mechanism solving high order partial derivatives of the strain formulation. The following articles present non-linear PRBM as part of their formulation: Reference [28] discusses conic section flexure hinges using Euler beam model and Castigliano's second theorem. Reference [29] develops an extension of the Frenet-Serret beam equations to apply it on the synthesis of CMs. Reference[30] introduces an analytical approach to corner filleted flexure hinges using the Castigliano's second theorem. In [31] a PRBM is developed and solved for the tip deflection of flexible beams under combined loads. It uses a numerical technique to solve the large - deflection Euler-Bernuolli beam equation. Reference [12] develops a synthesis and analysis PRBM for the limit positions of a four-bar mechanisms with an output compliant link (one end pinned to the coupler, one end fixed to the ground). The lumped compliance is modeled by non-linear beam theory, allowing for large non-linear deflections of the pinned end of the compliant link. The model only applies for a given topology. In [11] PRBM is enhanced to allow large deflections of elastic hinges. Four elastic hinges (leaf spring, cross, notch, and Haberland hinge) are modeled and a joint-based modular approach is obtained. The modeling technique reported reduces the time needed for off-line modeling and design but not enough for real-time control. Reference [32] presents the mathematical model for a 6 DOF compliant mechanism derived based on the second Castigliano's theorem. The forward and inverse analyses of an open loop compliant mechanism are discussed in [33], using numerical methods to solve large deformations of the mechanism. In [34] a mathematical dynamic model for compliant constant force compression mechanisms is developed based on large - deflection beam models.

In general, PRBM is useful to model lumped compliance. Models obtained with linear PRBM can be applied in real-time control but is restricted in precision engineering applications because of its low accuracy ([7, 11]). Non-linear PRBM is suitable for accurate modeling and design, but it is not computationally efficient for real-time control.

2.4.2 Topology Optimization

Topology optimization consists in finding the optimal lay-out of a loaded structure within a specified region and with specified performance criteria. In [35] the topology optimization method for designing compliant mechanisms is described. [36] proposes a honeycomb tessellation and material - mask overlay methods to obtain optimal single-material compliant topologies. Topology optimization methods based on material distribution are reported to be usually ill - posed [7]. Alternatives to this problem are proposed in the form of homogenization [37], the Solid Isotropic Material with Penalization method (SIMP) [38] and, level set methods [7]. In reference [39] the topology optimization method is performed to develop constant output force CMs for a given actuator characteristic. Reference [35] proposes a method for non-linear optimization based on geometric and material non-linearities to obtain a desired displacement under an specific load.

The topology optimization methods are limited to the design stage. The majority of the methods that use topology optimization for the synthesis of compliant mechanism are restricted to one operation point of the mechanism.

2.4.3 Numerical methods

The pseudo rigid body model (PRBM) works when parts of the structure analyzed are significantly weaker than others in the body. The weaker ones concentrate the movement. The stiffer ones are considered totally rigid. In addition, the weaker parts must have a geometry that accepts close forms of force - deformation equations. When PRBM is not applicable, Finite Element Analysis (FEA) are used for the analysis of CMs [11]. Reference [40] presents a procedure for the optimal design of flexural hinges for compliant micro-mechanisms. The optimal design is developed

by coupling a finite element model to an optimization algorithm. The optimization is intended to maximize the rotation of the hinges under kinematic and strain constrains of the material of the hinge. Because of its time expenses, a pure FEA modeling of CMs is restricted to the design stage of the mechanism, being excluded from the real-time control applications.

FEA, however, may be applied in a reduced manner for real-time Input / Output models of CMs. In [41] a methodology for finite element analysis of planar CMs is reported, with two main steps: 1- the properties of the hinges are determined by an independent 3D FEA, 2- these properties are incorporated into a general CM model by the use of equivalent beams. The methodology is reported to reduce the computational effort with respect to a model developed exclusively with FEA and is applicable in real-time control. Reference [42] presents the synthesis of compliant mechanisms using nonlinear FEA that appropriately accounts for large displacements. In order to model the mechanism it is necessary to specify its desired accuracy and prescribed force-deflection. Reference [43] describes the design of a robotic wrist able to perform spherical motions. The inverse and direct kinematics and the design of flexures of the spherical complaint mechanisms are computed by FEA. In [44] the stiffness properties of a notch hinge are computed using FEA relating the initial and final positions of the mechanisms under known loads. The procedure is only used to find the properties of the flexures and not to find an input / output model of the compliant mechanism. In [45] a synthesis method for spatial compliant mechanisms is proposed. The mechanisms are modeled as a set of connected three dimensional wide curves. A three dimensional wide curve is a spatial curve with variable cross section and multilayer materials. Deformation and performance of the mechanism are evaluated by an iso-parametric degenerate-continuum nonlinear finite elements procedure.

Numerical methods as FEA are useful in determining the deflection and stresses in compliant mechanisms. There are two main reasons for using these methods: (i). They are useful in validating or refining designs obtained using complementary methodologies as PRMB. (ii). To analyze compliant mechanisms that have a geometry that is not easily modeled using methods like the PRBM. Numerical methods are not useful directly to create input/output models of CMs.

2.4.4 Contribution of this Article

This article presents a new general procedure for modeling compliant mechanisms under quasi-static conditions by Computer Experiment Design methodology.

The proposed approach allows to model compliant mechanisms that have lumped or distributed compliance. The main advantages of the proposed approach with respect to traditional modeling methods (PRBM, topology optimization, FEA) are:

1. The methodology is general enough to cover both lumped and distributed compliant mechanisms.
2. The obtained input-output model is enough simple to be used in real-time control.
3. Real experimentation is replaced by computer simulations reducing costs in product development.

As an application of the methodology, the 6 DOF compliant mechanism HexFlex is modeled by finding an accurate model with respect to a FEA simulations.

2.5 Meta-modeling of complaint mechanisms methodology

In Meta-modeling of compliant mechanisms we are looking for a function that relates the input forces and torques (τ) with translations and rotations of the end-effector ($\mathbf{r}$) under quasi-static conditions:

$$f : \tau \rightarrow \mathbf{r} \tag{1}$$

$$\tau = \begin{bmatrix} \tau_1 & \tau_2 & \cdots & \tau_n \end{bmatrix}^T \tag{2}$$

$$\mathbf{r} = \begin{bmatrix} r_1 & r_2 & \cdots & r_m \end{bmatrix}^T \tag{3}$$

with $m \leq n$.

For an end-effector taking and arbitrary pose, we have $m = 6$. We assume that mechanisms are not redundant, then $m = n$.

To model compliant mechanisms under quasi-static condition using computer-based meta-models from computational experiments, the methodology presented in Fig. 1 is proposed, and summarized as follows:

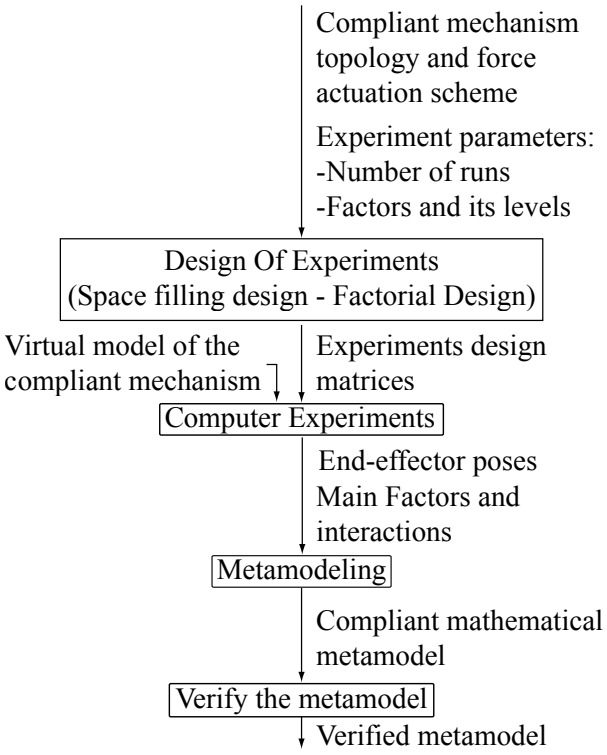

Figure 1: Methodology for force-displacement meta-modeling of compliant mechanisms

1. Define the compliant mechanism topology. The set of factor parameters is defined as the input forces and torque vector (τ).

2. Perform a virtual model of the compliant mechanism.

3. Use a Factorial Design Of Experiments (DOE) (*e.g.* Plackett Burman) to screen variables. The main factors and interactions are obtained by virtual experiments.

4. Use an Space Filling Design of Experiments (*e.g.* Uniform Design [46]) to fine-tune the mathematical model of the mechanism by virtual experiments.

5. Construct the surrogate model of the kinematics of the compliant mechanism.

6. Verify the accuracy of the meta-model using extra experiments [17].

In section 2.6 the proposed methodology is applied to obtain a mathematical meta-model of the HexFlex parallel compliant mechanism. The developed meta-model relates the actuator forces at the input ports with the position and orientation of the end-effector stage.

2.5.1 Scope of the Methodology

The presented methodology for modeling CMs is limited to:

1. CMs that allows small displacements of its end-effector.

2. Input forces and moments slowly varying in time (quasi-static conditions).

3. The model is restricted to the neighborhood of the the operation point for which was calculated.

4. Although the proposed methodology is general for compliant mechanisms, the obtained force-displacement models are specific for each analysis case.

In spite of this limitations, the proposed force-displacement modeling of CMs by Computer Design of Experiments has application for a wide range of applications because: most compliant mechanisms are designed for small displacements of its end-effector under quasi-static conditions, specially in compliant parallel nano-manipulating mechanisms.

Section 2.6 shows the meta-modeling of the HexFlex compliant mechanism under quasi-static conditions.

2.6 Force-displacement meta-modeling of the HexFlex parallel compliant mechanism

Applying the procedure described in section 2.5 the HexFlex parallel compliant mechanism is meta-modeled.

The meta-model of the HexFlex is developed in detail as follows: in section 2.6.1 the mechanism is described. The input factors (input forces) and its levels are determined. Section 2.6.2 develops the Fractional Design of Experiments to determine the main factors and interactions. Section 2.6.3 presents the Space Filling Design of experiments and the meta-modeling of the HexFlex CM. Finally, section 2.6.5 develop a validation of the obtained meta-model by comparison with FEA simulations.

2.6.1 CASE STUDY: HexFlex Parallel Compliant Mechanism

The topology and dimensions of the HexFlex are shown in Fig. 2. This mechanism allows the motion stage translation and rotation trough the X, Y and Z axes as shown in Fig 2.6.1. The HexFlex is composed by a triangular motion stage, three tabs to provide an interface with the actuators, and six connection beams between the motion stage and the grounded zone, Fig. 2(a).

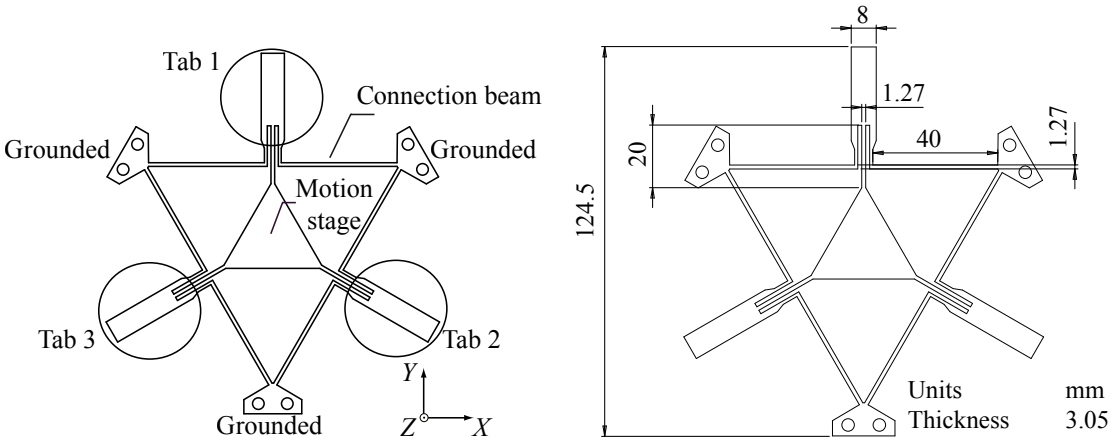

(a) HexFlex components

(b) HexFlex main dimensions

Figure 2: Six degree of freedom compliant mechanism [1]

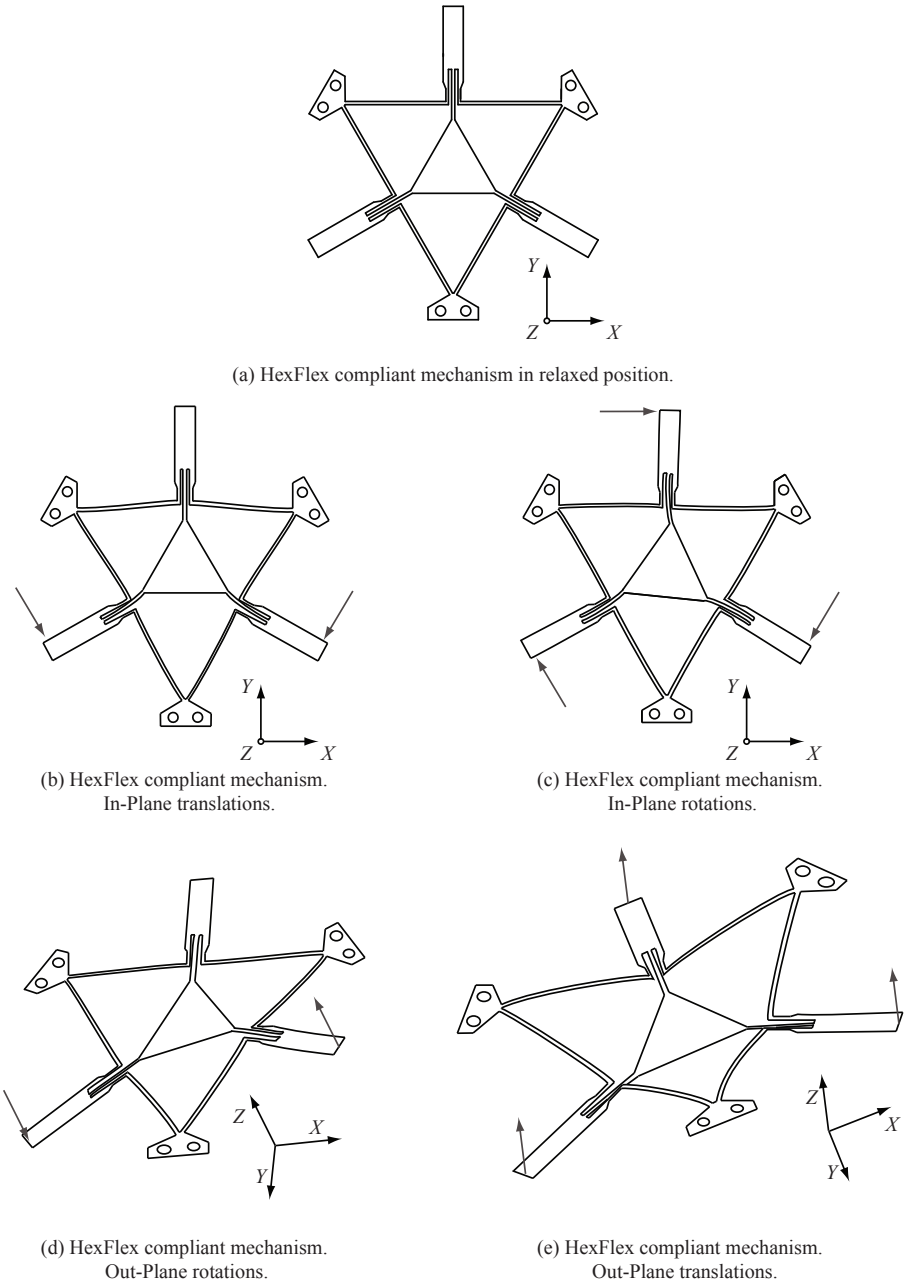

(a) HexFlex compliant mechanism in relaxed position.

(b) HexFlex compliant mechanism. In-Plane translations.

(c) HexFlex compliant mechanism. In-Plane rotations.

(d) HexFlex compliant mechanism. Out-Plane rotations.

(e) HexFlex compliant mechanism. Out-Plane translations.

Figure 3: Six degree-of-freedom complaint mechanism moves.

To control the motion stage there are two actuators in the external edge of each tab. For each tab, one actuator acts in direction parallel to the connection beams (called direction one and denoted D1) and, the other actuator acts perpendicular to the tab

(in Z direction, called direction two and denoted D2), Fig.4. Tabs are denoted T1, T2, T3. The motion of an specific actuator is denoted by the tab followed by the direction using the convention shown in Fig.4.

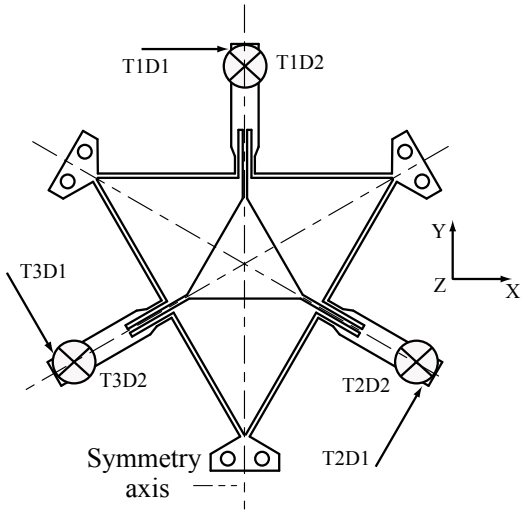

Figure 4: HexFlex actuators direction

The actuators used in the experiments allows a force of ± 1 N. The positive direction of actuators for D2 coincides with the direction in which Z is positive, and for D1 the positive direction of actuators is as shown in Fig. 4. Slowly varying in time forces are assumed for the experiments (quasi-static experiments). Planar and non-planar displacements may be made simultaneously. The material selected to model the mechanism is Aluminum 7075.

To define the meta-model function, the vector of input forces (τ) and pose of the end-effector ($\mathbf{r}$) are defined by:

$$\tau = \begin{bmatrix} \text{T1D1} & \text{T1D2} & \text{T2D1} & \text{T2D2} & \text{T3D1} & \text{T3D2} \end{bmatrix}^T \tag{4}$$

$$\mathbf{r} = \begin{bmatrix} x & y & z & \theta_x & \theta_y & \theta_z \end{bmatrix}^T \tag{5}$$

where the end effector pose (position and orientation) is defined by three translational components (x, y, z) and three differential Euler XYZ angles (θ_x, θ_y, θ_z), and the input forces correspond to the actuators in Tabs. Differential Euler angles

are commutative (the order of the x, y and z rotations do not affect the final orientation, [47]) The reference frame is assumed to be coincident with the center of the motion stage in its relaxed position, Fig. 5. A moving frame is attached to the motion stage center. In relaxed position the reference frame and the moving frame coincide.

Using the symmetry of the mechanism and the dimension shown on Fig. 2(b), a sixth part of the mechanism was modeled and meshed to made a geometric FEM model of the mechanism, Fig. 5(a). Using geometric transformations, the mechanism was completed developing a symmetrical mesh. Then the mesh was exported to ANSYS using quads shell elements to run the virtual design of experiments, Fig. 5(b). The computer experiments consist in given a set of input loads in the tabs, to obtain the position and orientation of the moving frame on the mechanism.

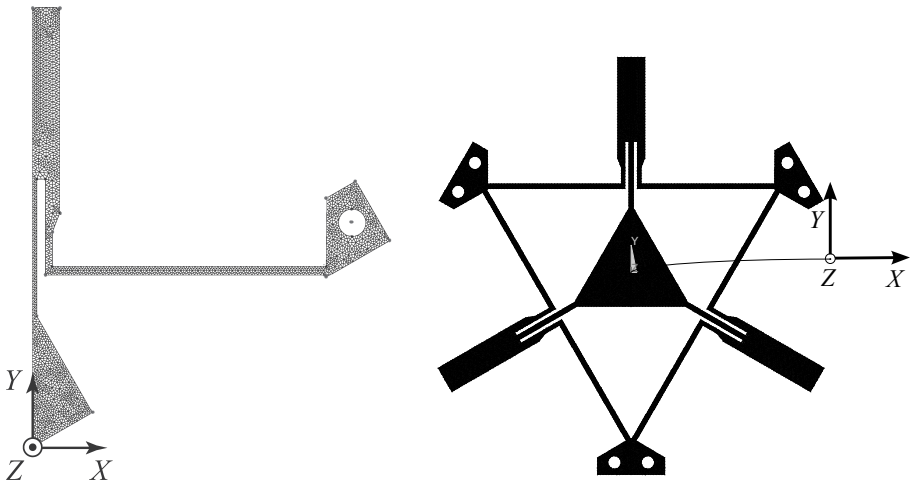

(a) Sixth part of the mesh (b) FEM model in ANSYS

Figure 5: Finite element method model of the HexFlex

For the Fractional Factorial and Space Filling Design Of Experiments the the high and low level of each factor defined by the designer [1] are displayed in Table 1. The factors or inputs of the experiments are defined by Eq. 4 and correspond with the actuation forces of the mechanism, which are the controllable variables of the experiment.

In design of experiments the factors correspond to the controllable input variables.

Factor	Low level	High level
T1D1	−1N	+1N
T1D2	−1N	+1N
T2D1	−1N	+1N
T2D2	−1N	+1N
T3D1	−1N	+1N
T3D2	−1N	+1N

Table 1: Studied Factors. Forces in Tabs of the HexFlex

In the case of the HexFlex the controllable input variables are the input forces at input ports.

In sections 2.6.2 and 2.6.3, the Factorial and Space Filling Design of experiments defining the meta-model of the HexFlex are developed.

2.6.2 Fractional Factorial Design of Experiments

To screen variables a Plackett Burman DOE [48, 49] with 12 runs is made. Plackett Burman designs are very economical and efficient DOE when only main effects are of interest. A script was developed to automatically generate the virtual experiments and its results. The design of experiments matrix and the results of each response are shown on Table 2.

Design Matrix						**Responses**					
T1D1	**T1D2**	**T2D1**	**T2D2**	**T3D1**	**T3D2**	x	y	z	θ_x	θ_y	θ_z
[N]	[N]	[N]	[N]	[N]	[N]	[μm]	[μm]	[μm]	[μrad]	[μrad]	[μrad]
1	−1	1	−1	−1	−1	115056	0,6	−862976	0,0001	−0,0001	3,10176
−1	−1	1	1	1	−1	−57529	99636,5	−287659	−39,3596	−68,0656	3,10183
1	−1	−1	−1	1	1	−3	−0,6	−287655	−39,2665	68,1194	−9,30545
−1	−1	−1	−1	−1	−1	−57525	−99636,5	−862976	0,0001	−0,0001	3,10186
1	1	−1	1	1	−1	−3	−0,6	287655	39,2665	−68,1194	−9,30545
1	1	1	−1	1	1	57525	99636,5	287659	39,3596	68,0656	−3,10186
−1	−1	−1	1	1	1	−115056	−0,6	287662	−78,6262	0,0539	−3,10176
−1	1	−1	−1	−1	1	−57525	−99636,5	287659	39,3596	68,0656	3,10186
−1	1	1	1	−1	1	3	0,6	862976	−0,0001	0,0001	9,30545
−1	1	1	−1	1	−1	−57529	99636,5	−287662	78,6262	−0,0539	3,10183
1	1	−1	1	−1	−1	57529	−99636,5	287655	39,2665	−68,1194	−3,10183
1	−1	1	1	−1	1	115056	0,6	287662	−78,6262	0,0539	3,10176

Table 2: Plackett-Burman design of experiments Matrix for Six factors and 12 runs

To analyze the results of the Plackett Burman DOE, a Pareto (Fig.7) and Half Normal Probability (HNP) plots are made (Fig.6). These analyses provide a simple way to examine the response variables (*i.e.* x, y, z, etc) and the relative importance of the factors and interactions of the experiment.

The Pareto charts results coincide with Half Normal Probability (HNP) showing that the main interactions are consequent with the symmetries on the topology of the mechanism (Fig. 4). The symmetries of the mechanism also made that some effects had the same influence value.

In addition to the Pareto charts and Half Normal Probability analysis, another way of looking at the resulting effects consists in using Lenths plot [50]. The absolute value of the alias of the effects are ordered in ascending order to calculate the median (ν). Once the median is calculated a pseudo-standard error (S_0) using the formula: $S_0 = 1.5\nu$. The pseudo-standard error serves to define the margin of error (ME), and the simultaneous margin of error, by using the 0.975-quantile and tg, $m/3$ of the t-student distribution allowing fractional degrees of freedom. The results for these analyses are displayed on Table 3:

	x [μm]	y [μm]	z [μm]	θ_x [μrad]	θ_y [μrad]	θ_z [μrad]
T1D2	0,17	0	575314	78,63	0,05	0
T2D2	0,17	0	575317	39,36	68,07	0
T3D2	0,17	0	575321	39,27	68,12	0
T2D1	57527,5	99637,1	0	0	0	6,2
T3D1	57531,5	99635,9	0	0	0	6,2
T1D1	115053,5	0	0	0	0	6,2
ν	19,63	0	287657	19,63	0,03	3,1
S_0	29,45	0	431485,5	29,45	0,04	4,65
ME	110,73	0	0	0	0	0
SME	265,34	0	0	0	0	0

Table 3: Lenths analysis of Six DOF HexFlex Mechanism

These analyses show conclusively and consistently which alias of the effects are active and which are not for the displacements in the x, y and z directions and the rotations in x, y and z. The main effects that affect each factor are:

1. x and θ_z are mainly affected by $T1D1$ $T2D1$ $T3D1$.
2. z and θ_x are mainly affected by $T1D2$ $T2D2$ $T3D2$.
3. y is mainly affected by $T2D1$ $T3D1$.
4. θ_y is mainly affected by $T2D2$ $T3D2$.

Also, it is evident that to obtain in-plane displacements (x, y, θ_z) actuators should act in direction one (D1) and, out-of-plane displacements (z, θ_x, θ_y) are generated when actuators acts in direction two (D2).

2.6.3 Space Filling design of experiments and Meta-model of the HexFlex

To generate a valid meta-model of the HexFlex an Uniform DOE [51] with six factors and six levels is used (Table 1). An Uniform Design is a modification of fractional factorial designs that provides scatter design points in the experimental domain space. The design matrix and the output displacements found using Ansys (FEA) are shown on Table 4.

2.6.4 Meta-modeling HexFlex Parallel Complaint Mechanism

After running the space filling design of experiments (Sec.2.6.3), the next step consist on choosing an appropriate approximation model.

Low-order polynomials have been used effectively for building approximations in a variety of applications including force-displacement modeling [52]. Here a second order polynomial with interactions is used for meta-modeling an input-output of the HexFlex.

The chosen polynomial model for the input-output meta-model of the HexFlex is shown on Eq. 6.

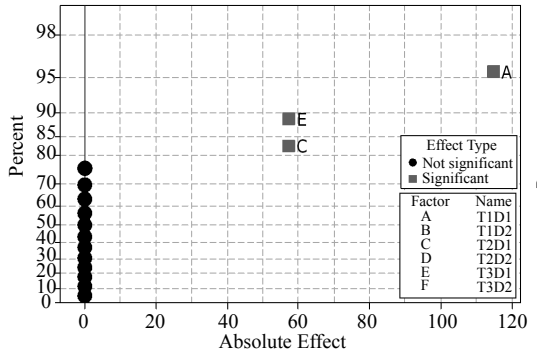

(a) Half Normal Plot for x translation

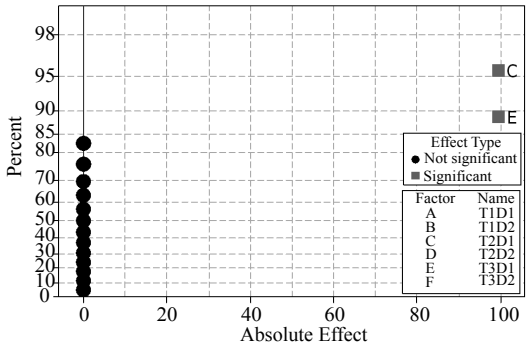

(b) Half Normal Plot for y translation

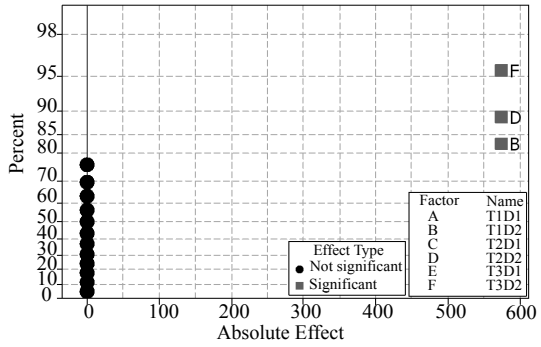

(c) Half Normal Plot for z translation

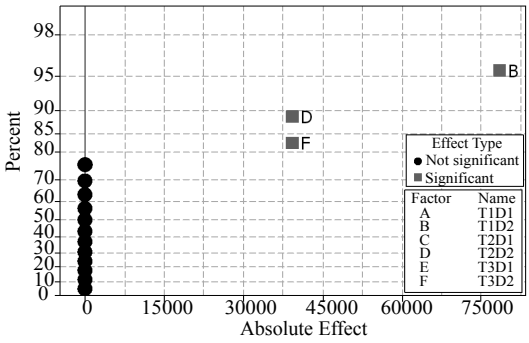

(d) Half Normal Plot for θ_x translation

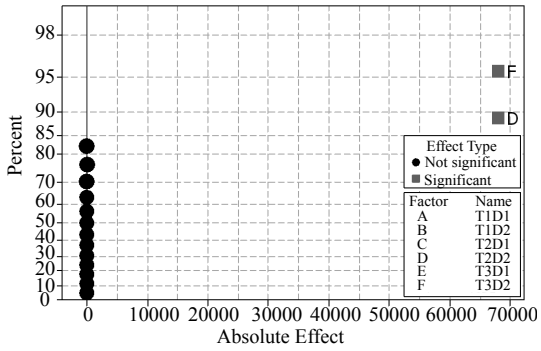

(e) Half Normal Plot for θ_y translation

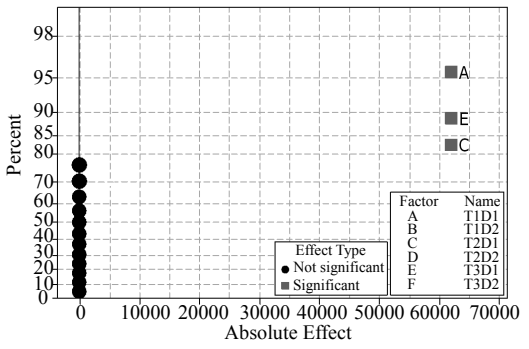

(f) Half Normal Plot for θ_z translation

Figure 6: Half Normal Probability Plots. Placket Burman design of experiments for 12 runs and 6 factors for HexFlex quasi-static conditions

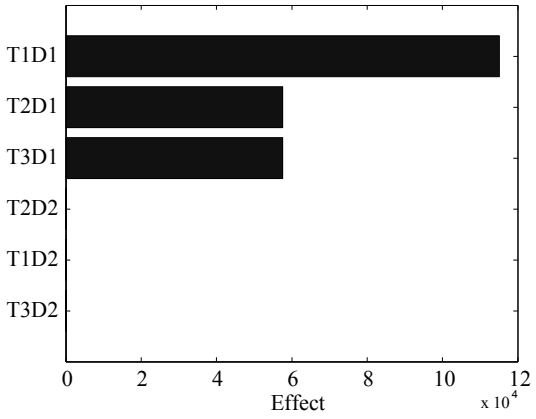

(a) Pareto effects for x translation

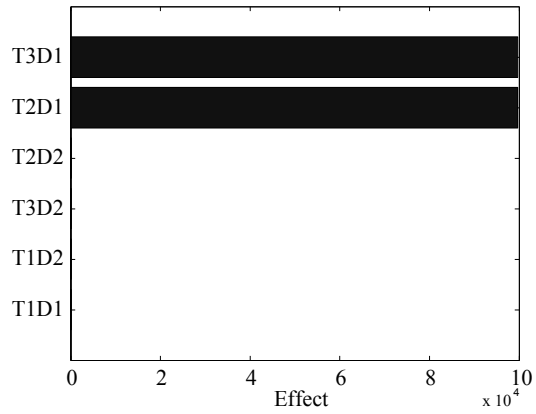

(b) Pareto effects for y translation

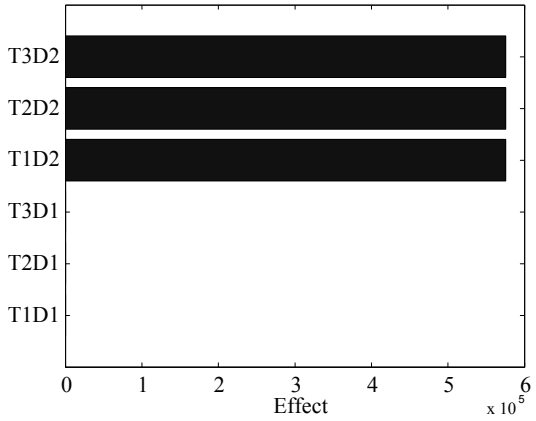

(c) Pareto effects for z translation

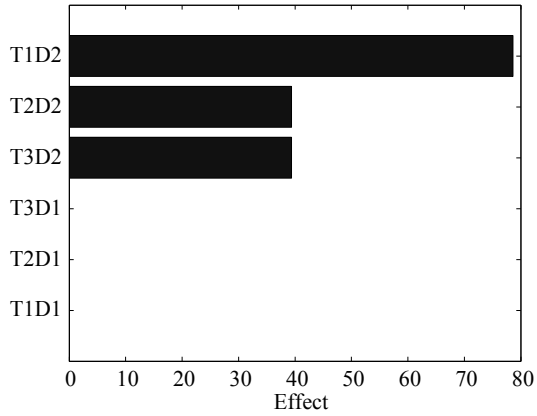

(d) Pareto effects for θ_x translation

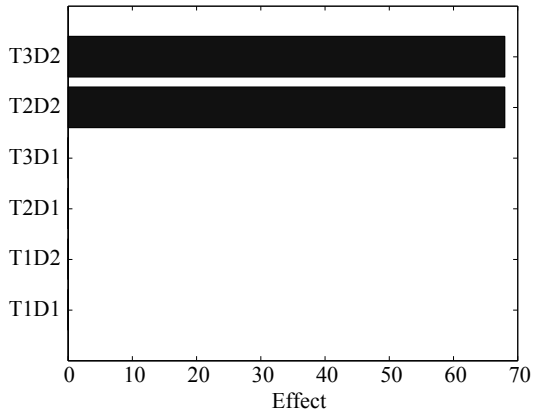

(e) Pareto effects for θ_y translation

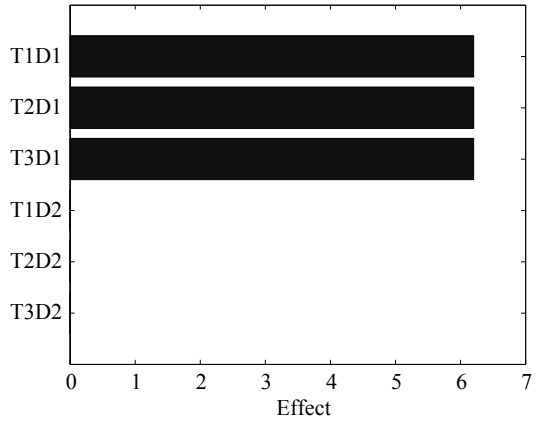

(f) Pareto effects for θ_z translation

Figure 7: Pareto Charts. Placket Burman design of experiments for 12 runs and 6 factors for HexFlex quasi-static conditions

Design Matrix						**Responses**					
T1D1	**T1D2**	**T2D1**	**T2D2**	**T3D1**	**T3D2**	x	y	z	θ_x	θ_y	θ_z
[N]	[N]	[N]	[N]	[N]	[N]	[μm]	[μm]	[μm]	[μrad]	[μrad]	[μrad]
0,6	-0,2	-1	-1	1	-0,2	-23	0	-403,37	15723,33	27294,4	-8057,19
-0,6	-0,6	0,2	1	-1	0,2	0	-39,85	172,88	-47310,09	-27294,38	5583,32
-0,2	0,2	-0,2	-1	-1	0,6	11,5	-59,78	-57,63	15769,99	54588,86	3098,05
-1	-0,2	1	0,6	-0,2	1	-23,01	39,85	403,37	-39390,09	13647,29	6831,66
1	0,2	1	1	0,6	0,2	69,02	79,71	403,37	-15723,33	-27294,4	-1883,93
-1	-1	-0,2	-1	-0,2	-1	-57,52	-19,93	-864,35	-116,71	-0,06	3120,86
-0,6	0,2	-1	1	0,2	0,6	-69,02	-39,85	518,61	-23596,69	-13647,16	-1838,28
0,6	-0,6	0,6	0,6	0,2	-1	46,01	39,85	-288,11	-15816,67	-54588,89	-635,59
-1	1	-0,6	-0,2	-0,6	0,2	-57,52	-59,78	288,1	39483,43	13647,2	3120,87
0,2	1	0,2	1	-0,2	-0,6	23,01	0	403,35	31610,14	-54588,88	612,76
-0,6	0,6	0,2	-1	0,2	1	-34,51	19,93	172,86	23690,01	68236,09	1872,51
1	-1	-0,2	0,6	-0,6	-0,2	69,02	-39,85	-172,86	-47356,77	-27294,41	-1883,92
-1	0,6	-0,2	0,6	0,6	-0,2	-80,53	19,93	288,11	15816,74	-27294,44	646,99
-1	0,2	0,6	-0,6	1	-0,6	-69,02	79,71	-288,12	31516,73	-0,05	1883,92
1	1	0,6	-1	-0,2	0,2	80,52	19,93	57,61	55230,1	40941,61	-646,99
1	0,6	-1	0,2	0,2	-0,6	23,01	-39,85	57,61	31563,44	-27294,47	-6831,66
0,2	1	-0,6	-0,6	0,6	-1	-23,01	0	-172,89	70976,84	-13647,3	-4334,97
0,6	0,6	-0,6	0,6	-1	1	46,02	-79,71	633,86	-7803,34	13647,27	-635,57
0,2	0,2	0,6	0,2	-0,6	-0,2	46,01	0	57,62	7896,7	-13647,22	3086,63
0,6	-0,2	0,2	-0,6	-1	-0,6	69,02	-39,85	-403,37	15723,35	-0,04	1838,29
0,6	-0,6	1	-0,6	-0,6	0,6	80,52	19,93	-172,86	-23690,1	40941,67	3075,22
0,2	-1	0,2	0,2	1	1	-11,5	59,78	57,64	-63103,51	27294,51	-3098,05
-0,2	0,6	1	-0,2	-1	-1	46,01	0	-172,88	47310,13	-27294,5	6808,84
-0,6	-1	1	-0,2	0,6	-0,2	-23,01	79,71	-403,35	-31610,1	0	3109,44
-0,2	-0,6	-0,6	-0,6	0,2	0,2	-34,51	-19,93	-288,11	-15816,74	27294,44	-1849,69
-0,2	-0,6	-0,6	1	1	-0,6	-57,52	19,93	-57,62	-31563,37	-54588,85	-4323,57
-0,6	-0,2	-1	0,2	-0,6	-1	-46,01	-79,71	-288,12	7850,04	-40941,69	635,59
-0,2	1	0,6	0,2	1	0,6	-23,01	79,71	518,6	23736,74	13647,23	-612,77
1	-0,2	-0,2	-0,2	0,6	1	34,51	19,93	172,88	-23643,42	40941,7	-5594,73
0,2	-1	-1	-0,2	-0,2	0,6	-11,5	-59,78	-172,85	-47356,81	27294,48	-3098,03

Table 4: Uniform design of experiments and results of the Experiments

$$\mathbf{r}_i \quad = \quad \beta_0 + \sum_{i=1}^{k} \beta_i \tau_i + \sum_{i=1}^{k} \beta_{ii} \tau_i^2 + \sum_{i=1}^{k} \sum_{j=1}^{k} \beta_{ij} \tau_i \tau_j \tag{6}$$

where: $i = 1, \ldots, 6$,$j = 1, \ldots, 6$, $i < j$, and τ and $\mathbf{r}$ are defined in Eq. 4 and Eq. 5 respectively.

From the Placket-Burman design of experiments analysis, it is evident that interactions are not important on the behavior of the mechanism and could be neglected from Eq. 6. Also from preliminary experiments it is determined that the quadratic terms of Eq. 6 do not influence the behavior of the mechanism and are neglected too.

The resulting simplified model of an force-displacement meta-model of the HexFlex is shown on Eq. 7.

$$\begin{bmatrix} x & y & z & \theta_x & \theta_y & \theta_z \end{bmatrix}^T = S_T \begin{bmatrix} \text{T1D1} & \text{T1D2} & \text{T2D1} & \text{T2D2} & \text{T3D1} & \text{T3D2} \end{bmatrix}^T \quad (7)$$

where, the matrix S_T represents the input-output matrix of the mechanism. Each term of the matrix S_T is found using a penalized least squares regression [53, 54] (Eq.8). Units associated to the elements of the matrix S_T for the HexFlex are as follow: rows 1 to 3 μm/N and rows 3 to 6 μrad/N.

$$S_T = \begin{vmatrix} 57.53 & 0 & 28.76 & 0 & -28.76 & 0 \\ 0 & 0 & 49.82 & 0 & 49.82 & 0 \\ 0 & 287.66 & 0 & 287.66 & 0 & 287.66 \\ 0 & 39313.03 & 0 & -19679.85 & 0 & -19633.3 \\ 0 & 0 & 0 & -34032.01 & 0 & 34060.19 \\ -3101.84 & 0 & 3101.79 & 0 & -3101.81 & 0 \end{vmatrix} \quad (8)$$

The inverse model is found from Eq. 9.

$$\begin{bmatrix} \text{T1D1} & \text{T1D2} & \text{T2D1} & \text{T2D2} & \text{T3D1} & \text{T3D2} \end{bmatrix}^T = S_T^{-1} \begin{bmatrix} x & y & z & \theta_x & \theta_y & \theta_z \end{bmatrix}^T \quad (9)$$

2.6.5 Validation of the HexFlex Meta-model

To validate the accuracy of the the meta-model, 1000 random experiments with an uniform distributions and factor levels between -1N and 1N are made. The found forward model is used to compare the pose estimations using meta-modeling against

the FEA software Ansys. The precision of the model is calculated using three error criteria: 1. the maximum absolute error ($MAXABS$ Eq. 10), 2. the relative error between the meta-model and the FEA model, and 3. the root mean square error ($RMSE$ Eq. 11) over the set of experiments. The $MAXABS$ and relative % of error, allows to calculate the local error. The $RMSE$ provides good estimate of the global error. The error between meta-model predictions and Ansys results is shown in Table 5. The deformed shape of the mechanism for one of the experiments made to validate the accuracy of the meta-model is in Fig 8.

$$MAXABS = max\left\{\left|\psi_i - \widehat{\psi_i}\right|\right\}_{i=1,\ldots,n_{error}} \tag{10}$$

$$RMSE = \sqrt{\frac{\sum_{i=1}^{n_{error}}(\psi_i - \widehat{\psi_i})^2}{n_{error}}} \tag{11}$$

	$MAXABS$	MAX $\%error$	$RMSE$
x [μm]	4,01E-04	1,08E-03	8,67E-05
y [μm]	4,18E-04	3,59E-04	2,07E-05
z [μm]	2,85E-04	2,41E-04	4,19E-05
θ_x [μrad]	2,41E-02	2,26E-03	9,78E-04
θ_y [μrad]	4,16E+00	6,21E-01	5,57E-03
θ_z [μrad]	2,10E-02	2,30E-03	2,23E-03

Table 5: Error between meta-model estimations and Ansys simulations for 1000 random experiments with uniform distribution.

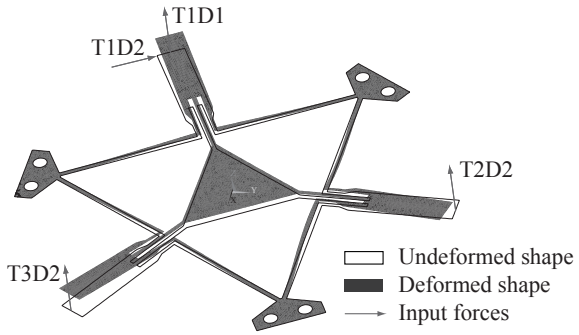

Figure 8: Deformed shape of HexFlex for one meta-model validation experiment.

2.7 Conclusions

This article presents a computer-based meta-modeling methodology for force-displacement modeling of compliant mechanisms under quasi-static conditions using Design of Computer Experiments. The methodology is applied to obtain a force-displacement model of the six degrees of freedom HexFlex compliant mechanism. To obtain the meta-model of the HexFlex, virtual experiments based on Plackett-Burman and Uniform Design of experiments are performed using the Finite Element Method (FEM). The obtained meta-model of the HexFlex is linear for the movement range of the mechanism. The accuracy of the meta-model was calculated with respect to a FEA-based model running a set of 1000 computer experiments with random uniform distribution over the allowable range of the force inputs (-1 N, 1 N). Three error criteria were calculated in each displacement direction ($x,\ y,\ z,\ \theta_x,\ \theta_y,\ \theta_z$): 1. the maximum absolute error (local error measurement), 2. the relative error between the meta-model and the FEA model, and 3. the root mean square error over the set of experiments (global error measurement). The maximum linear absolute error was founded in the y direction ($4.18 \exp -04 \mu$m). We compare this error with a manufacturing tolerance ISO h6 calculated on a shaft of nominal diameter 50 mm ($50mm^{+0}_{-19}\mu$m) founding the error as acceptable. The maximum relative error was founded in the θ_y direction (0.621%). This error level represents a better accuracy than the reported by P. A. Petri in [55]. In [55] the mechanism is analyzed using a virtual method based on Euler beam equations and the results are also compared with a FEA software founding a maximum relative error of 3%. Performing Factorial Designs of Experiments it was possible to identify characteristics of the behavior of the mechanism, such as the precence of symmetries in the actuation and the quasi-static behavior of the mechanism. To fine tune the model of the mechanism an Uniform Design of experiments was employed. The mechanism was modeled using a low-order polynomial, because of its quasi-static behavior and small displacements. The founded model allows to have an input/output model of the mechanism giving a transfer function for developing model-based control, reducing costs of experimentation and product development.

3 KINEMATIC IDENTIFICATION OF PARALLEL MECHANISMS BY A DIVIDE AND CONQUER STRATEGY

3.1 CONTEXT

Since 2007 the CAD CAM CAE Laboratory at EAFIT University, under my coordination, started the research project **GEOMETRIC ERROR MODELING IN MECHANISMS**. The goal of the project is to predict quasi-static deformations of mechanisms. Two types of deformations are considered: (1) Non-intentional and (2) Intentional. In traditional (kinematic joint-based) mechanisms the deformation is non-intentional and it is in general considered as negative. In contrast, there are mechanisms in which the deformation is intentional. In these mechanisms (called compliant) the functioning is precisely allowed by the deformation, since there are no kinematic joints (prismatic, revolute, spheric, etc.).

The goal of this chapter is to contribute to the research in positional errors in parallel mechanisms.

Parallel mechanisms are an instance of closed-loop mechanism recognized to have theoretical advantages with respect to their serial (open-loop) counterparts, specially for high accuracy and high speed tasks: (1) stiffer structure and, (2). reduced inertia of the links. However, the theoretical level of accuracy of parallel mechanism has not been reached, delaying a intensive use of such mechanisms for automated tasks. A recognized problem for this lack is that the accuracy of parallel mechanisms critically depends on the knowledge of the kinematic model that governs the control system. Therefore, one effective way to improve the accuracy of parallel mechanisms is to update its kinematic model with accurately estimated parameters.

This chapter aims to contribute to the kinematic identification of parallel mechanisms by a new kinematic identification of parallel mechanisms protocol based on inverse kinematics modeling and a divide and conquer method.

With respect to traditional identification methods, our divide and conquer method

has the following goals: (1) The optimization of the identification poses by the independent identification of reduced sets of parameters (the sets corresponding to each leg), (2) The improving of the numerical efficiency of the identification algorithms by the independent identification of the parameters of each leg and, (3) better Improvement of the end-effector accuracy after calibration with respect to other methods.

The content of this chapter corresponds to the article "Kinematic Identification of Parallel Mechanisms by a Divide and Conquer Strategy" by S. Durango, D. Restrepo, and O. Ruiz, accepted for publication in ICINCO 2010- 7th International Conference on Informatics in Control, Automation and Robotics. 15-18 June, 2010. Funchal, Madeira Portugal.

As co-authors of such publication, we give our permission for this material to appear in this document. We are ready to provide any additional information on the subject, as needed.

Prof. Dr. Eng. Oscar E. Ruiz
oruiz@eafit.edu.co
Coordinator CAD CAM CAE Laboratory
EAFIT University, Medellin, COLOMBIA

M.Sc. Sebastian Durango
sdurang1@eafit.edu.co
PhD student at CAD CAM CAE Laboratory
EAFIT University, Medellin, COLOMBIA

3.2 Abstract

This paper presents a Divide and Conquer strategy to estimate the kinematic parameters of parallel symmetrical mechanisms. The Divide and Conquer kinematic identification is designed and performed independently for each leg of the parallel mechanism. The estimation of the kinematic parameters is performed using the inverse calibration method. The identification poses are selected optimizing the observability of the kinematic parameters from the Jacobian identification matrix. With respect to traditional identification methods the main advantages of the proposed Divide and Conquer kinematic identification strategy are: (i) reduction of the kinematic identification computational costs, (ii) improvement of the numerical efficiency of the kinematic identification algorithm and, (iii) improvement of the kinematic identification results. The contributions of the paper are: (i) The formalization of the inverse calibration method as the Divide and Conquer strategy for the kinematic identification of parallel symmetrical mechanisms and, (ii) a new kinematic identification protocol based on the Divide and Conquer strategy. As an application of the proposed kinematic identification protocol the identification of a planar 5R symmetrical mechanism is (virtually) developed. The performance of the calibrated mechanism is evaluated by updating the kinematic models with the estimated parameters and developing kinematic simulations.

Nomenclature

g	-	Inverse kinematics function of a parallel mechanism.
k	-	Active joint gain.
n	-	Degrees of freedom of a mechanism.
n_{limbs}	-	Number of legs in a parallel mechanism.
$\mathbf{q}$	-	Active joint variables vector.
$\mathbf{r}$	-	End-effector pose (position and orientation) vector.
C	-	Kinematic identification matrix.
N	-	Number of measured configurations for the kinematic identification of a parallel mechanism.
$\mathbf{R}$	-	Set of end-effector configurations.
$\mathbf{Q}$	-	Set of active joint variables.
γ	-	Active joint offset.
φ	-	Kinematic parameters of a mechanisms.
σ	-	Standard deviation.

3.3 Introduction

In mechanisms and manipulators the accuracy of the end-effector critically depends on the knowledge of the kinematic model governing the control model [56]. Therefore, to improve the accuracy of a mechanism its kinematic parameters have to be precisely estimated [57]. The process of estimating the kinematic parameters and updating the kinematic model is formally known as kinematic identification or kinematic calibration [58].

Kinematic identification is an instance of the robot calibration problem. The estimation of rigid-body inertial parameters and the estimation of sensor gain and offset are instances of calibration problems at the same hierarchical level of the kinematic calibration problem [59].

This paper is devoted to the kinematic identification of parallel symmetrical mechanisms. Parallel mechanisms are instances of closed-loop mechanisms typically formed by a moving platform connected to a fixed base by several legs. Each leg is a kinematic chain formed by a pattern of links, actuated and passive joints relating the moving platform with the fixed base. If the pattern of joints and links is the same for each leg and each leg is controlled by one actuator, then the parallel mechanism is called symmetrical [60]. Most of the industrial parallel mechanisms can be classified as parallel symmetrical mechanisms.

For parallel mechanisms the kinematic identification is usually performed minimizing an error between the measured joint variables and their corresponding values calculated from the measured end-effector pose through the inverse kinematic model [56, 57]. This method is preferred for the identification of parallel mechanisms because:

1. Inverse kinematics of parallel mechanisms is usually derived analytically avoiding the numerical problems associated with any forward kinematics solution [56, 57].

2. The inverse calibration method is considered to be the most numerically efficient among the identification algorithms for parallel mechanisms [57, 61], and

3. With respect to forward kinematic identification no scaling is necessary to balance the contribution of position and orientation measurements [56].

In the case of parallel symmetrical mechanisms the inverse kinematic modeling can be formulated using independent loop-closure equations. Each loop-closure equation relates the end-effector pose, the geometry of a leg, and a fixed reference frame. In consequence, an independent kinematic constraint equation is formulated for each leg forming the mechanism. For the case of parallel symmetrical mechanisms the set of constraint equations is equal to the number of legs and to the number of degrees of freedom of the mechanisms. Each kinematic constraint equation can be used for the independent identification of the parameters of the leg correspondent to the equation.

The independent identification of the kinematic parameters of each leg in parallel mechanisms allows to improve:

1. The numerical efficiency of the identification algorithm [56], and
2. The kinematic calibration performance by the design of independent experiments optimized for the identification of each leg.

The independent identification of leg parameters in parallel mechanisms was sketched in [56] and developed for the specific case of Gough platforms in [62, 63]. However, the idea of the independence in the kinematic identification of each leg in a parallel mechanism is not completely formalized.

This article presents a contribution to the improvement of the pose accuracy in parallel symmetrical mechanisms by a kinematic calibration protocol based on inverse kinematic modeling and a divide and conquer strategy. The proposed divide and conquer strategy takes advantage of the independent kinematic identification of each leg in a parallel mechanism not only from a numerical stand point but also from the selection of the optimal measurement set of poses that improves the kinematic identification of the parameters of the leg itself.

The layout for the rest of the document is as follows: section 3.4 develops a literature review on the inverse calibration of parallel mechanisms method, section

3.5 presents the divide and conquer identification of parallel mechanisms strategy, section 3.6 develops a kinematic identification of parallel mechanisms protocol, section 3.7 presents the simulated kinematic identification of a planar 5R symmetrical mechanism using the identification protocol, finally, in section 3.8 the conclusions are developed.

3.4 Literature review

The modeling of mechanical systems include the design, analysis and control of mechanical devices. An accurate identification of the model parameters is required in the case of control tasks [59]. Instances of models of mechanical systems includes kinematic, dynamic, sensor, actuators and flexibility models. For parallel mechanisms updating the kinematic models with accurately estimated parameters is essential to achieve precise motion at high-speed rates. This is the case when parallel mechanisms are used in machining applications [57].

The inverse calibration method is accepted as the natural [57, 56] and most numerically efficient [61] among the identification algorithms for parallel mechanisms. The inverse calibration method is based on inverse kinematic modeling and a external metrological system. The calibration is developed minimizing an error residual between the measured joint variables and its estimated values from the end-effector pose though the inverse kinematic model. The derivation of the inverse kinematic model of parallel mechanisms is usually straightforward obtained [58]. Kinematic identification of parallel mechanisms based on inverse kinematics and the use of external metrology is reported in: Systematic approaches [58, 57, 64], calibration of hexapod mechanisms [56, 65, 66, 67], calibration of parallel mechanisms based machine-tools [68, 69], calibration of an orthoglide parallel mechanism [70], calibration of redundant parallel mechanisms [4], calibration of a microparallel mechanism [71], calibration of parallel mechanisms based on inverse kinematics singularities (type 2 singularities) [72], calibration of parallel mechanisms with Denavit and Hartenberg kinematic modeling [73], identifiability of kinematic parameters [74], and vision based identification [75].

For the Divide and Conquer kinematic calibration strategy we adopt the inverse calibration method. The method takes advantage of an intrinsic characteristic of paral-

lel mechanisms: the straightforward calculation of the inverse kinematics. However, not all the intrinsic characteristics of parallel mechanisms are exploited. Specifically, [56, 76] reported that for parallel mechanism, methods based on inverse kinematics allow to identify error parameters of each leg of the mechanism independently. The independent parameter identification of each leg is reported to improve the numerical efficiency of the kinematic identification algorithm, [56]. However, it is not reported a general kinematic identification strategy based on the independent identification of the legs and its advantages with respect to traditional identification methods.

This article presents a contribution to the kinematic calibration of parallel mechanisms developing a kinematic identification protocol based on the inverse calibration method and the independent identification of the parameters of each leg (Divide and Conquer strategy).

With respect to traditional identification methods, our Divide and Conquer strategy has the following advantages:

1. The identification poses can be optimized to the identification of reduced sets of parameters (the sets corresponding to each leg),
2. The independent identification of the parameters of each leg improves the numerical efficiency of the identification algorithms, and
3. By (1) and (2) the identified set of parameters is closer to the real (unknown) set of parameters than sets identified by other traditional calibration methods.

The divide and Conquer strategy for the independent kinematic identification of the parameters of each leg in a parallel symmetrical mechanism is presented in section 3.5.

3.5 Divide and Conquer Identification Strategy

Parallel symmetrical mechanisms satisfy [60]:

1. The number of legs is equal to the number of degrees of freedom of the end-effector.

2. All the legs have an identical structure. This is, each leg has the same number of active and passive joints and the joints are arranged in an identical pattern.

In a practical way, the definition of parallel symmetrical mechanism covers most of the industrial parallel structures. For parallel symmetrical mechanisms the kinematic identification by inverse kinematics and a divide and conquer strategy is stated as:

Given

1. A set of nominal kinematic parameters (φ) of the mechanism in terms of the parameters of the individual legs (φ_κ), each leg having n_κ parameters to be identified:

$$\begin{aligned} \varphi_\kappa &= \begin{bmatrix} \varphi_{\kappa,1} & \dots \varphi_{\kappa,n_\kappa} \end{bmatrix}^T, \\ \kappa &= 1, 2, \dots, n_{limbs}. \end{aligned} \tag{12}$$

2. An inverse kinematic function g_κ relating the κth active joint variable ($\mathbf{q}_\kappa$) with the end-effector pose ($\mathbf{r}$). For the jth pose of the mechanism the inverse function of the κth leg is defined to be:

$$\begin{aligned} g_\kappa^j &: \varphi_\kappa \times \mathbf{r}^j \rightarrow \mathbf{q}_\kappa^j, \\ \kappa &= 1, 2, \dots, n_{limbs}, \\ j &= 1, 2, \dots, N. \end{aligned} \tag{13}$$

3. n_{limbs} sets of N measured end-effector configurations. The κth set ($\hat{\mathbf{R}}_\kappa$) is for the identification of the κth leg.

$$\begin{aligned} \hat{\mathbf{R}}_\kappa &= \begin{bmatrix} \hat{\mathbf{r}}_\kappa^1 & \cdots & \hat{\mathbf{r}}_\kappa^N \end{bmatrix}^T, \\ \kappa &= 1, 2, \dots n_{limbs}. \end{aligned} \tag{14}$$

4. A set of measured input variables ($\hat{\mathbf{Q}}_\kappa$) corresponding to each set of end-effector

measurements ($\hat{\mathbf{R}}_\kappa$):

$$\begin{aligned} \hat{\mathbf{Q}}_\kappa = \begin{bmatrix} \hat{\mathbf{q}}_\kappa^1 & \cdots & \hat{\mathbf{q}}_\kappa^N \end{bmatrix}^T, \\ \kappa = 1, 2, \ldots n_{limbs}. \end{aligned} \tag{15}$$

Goal

To find the set of unknown (real) kinematic parameters ($\bar{\varphi}_\kappa$) that minimizes an error between the measured joint variables ($\hat{\mathbf{Q}}_\kappa$) and their corresponding values ($\bar{\mathbf{Q}}_\kappa$) estimated from the measured end-effector pose by the inverse kinematic model g_κ. The problem can be formally stated as the following non-linear minimization problem:

$$\begin{aligned} \bar{\varphi}_\kappa : \sum_{j=1}^{N} \left\| \hat{\mathbf{Q}}_\kappa - \bar{\mathbf{Q}}_\kappa \left(\hat{\mathbf{R}}_\kappa, \varphi_\kappa \right) \right\|^2 \text{ is minimum,} \\ \text{subject to : } \mathbf{R}_\kappa \subset \mathbf{W}_\mathbf{R}, \\ \mathbf{W}_\mathbf{R} \text{ is the usable end} - \text{effector workspace,} \\ \kappa = 1, 2, \ldots, n_{limbs}. \end{aligned} \tag{16}$$

The optimization problem is constrained by the workspace of the mechanism. The usable workspace is defined as the workspace without singularities by [77].

A kinematic identification of parallel symmetrical mechanisms protocol based on the Divide and Conquer identification strategy is developed in section 3.6.

3.6 Kinematic Identification Protocol

Based on the Divide and Conquer strategy for the kinematic identification of parallel symmetrical mechanisms (section 3.5) the following kinematic identification protocol (Fig. 9) is proposed.

1. Given the nominal parameters of the κth leg (φ_κ, Eq. 12) and the correspondent inverse kinematic function (g_κ, Eq. 13) to calculate the κth Jacobian

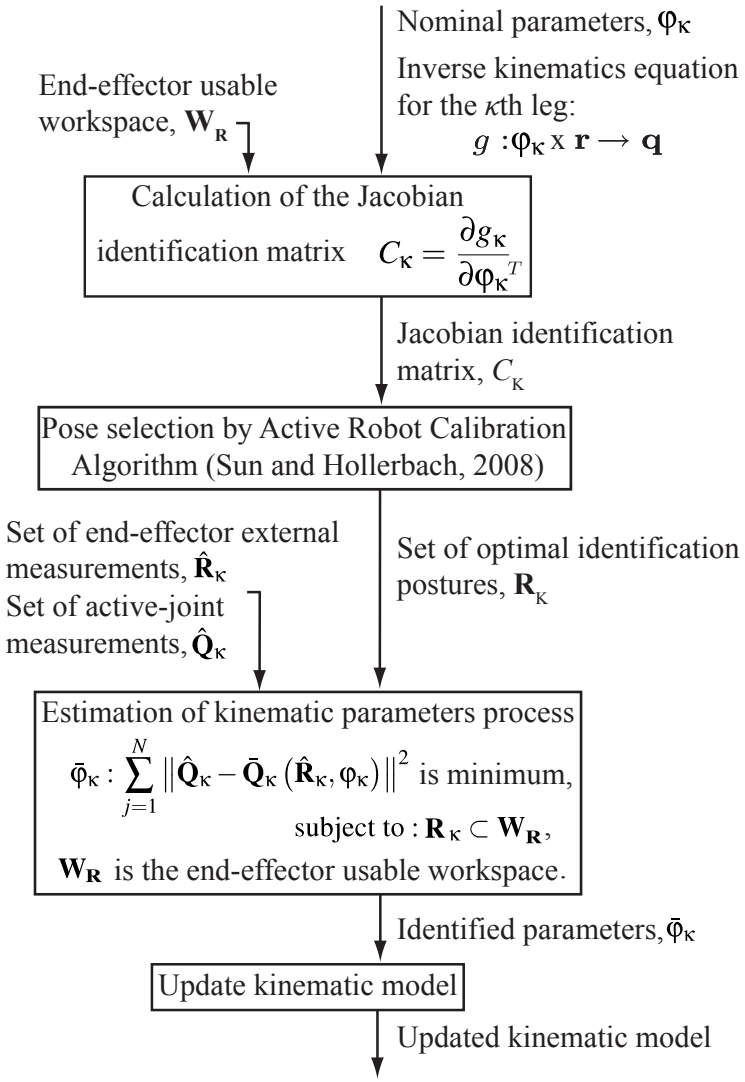

Figure 9: Kinematic identification of parallel symmetrical mechanisms protocol.

identification matrix of a representative set of postures of the usable workspace:

$$C_\kappa = \frac{\partial g_\kappa}{\partial \varphi_\kappa^T}. \tag{17}$$

2. Given the Jacobian identification matrix calculated in the first step to select an optimal set of postures ($\mathbf{R}_\kappa$) for the kinematic identification of the κth leg. The set of postures is selected searching the improvement of the observability of the set of parameters φ_κ. To select the poses we adopt the active calibration

algorithm developed by [78] that reduces the complexity of computing an observability index reducing computational time for finding optimal poses. The optimized identification set of postures is then defined by:

$$\begin{aligned} \mathbf{R}_\kappa &: O_1(C_\kappa) \text{ is maximal}, \\ O_1(C_\kappa) &= \frac{\sqrt[n_\kappa]{s_1 \ s_2 \cdots s_{n_\kappa}}}{n_\kappa}, \\ \mathbf{R}_\kappa &\subset \mathbf{W}_\mathbf{R}, \\ \kappa &= 1, 2, \ldots, n_{limbs}, \end{aligned} \tag{18}$$

were O_1 is an observability index of the total identification matrix (C_κ) of the κth leg, n_κ is the number of parameters to be identified in the κth leg, and $s_1,\ s_2\ \ldots, s_{n_\kappa}$ are the singular values of the identification matrix C_κ. As a rule of thumb, in order to suppress the influence of measurement noise, the number of identification poses should be two or three times larger than the number of parameters to be estimated [79].

3. Given the optimized set of identification postures obtained in the second step and the correspondent sets of active joint ($\hat{\mathbf{Q}}_\kappa$) and end-effector ($\hat{\mathbf{R}}_\kappa$) measurements to solve the optimization problem defined on Eq. 16 for the identification of the kinematic parameters (φ_κ) of the κth leg.

4. Given the identified set of parameters of the κth leg obtained in the third step to update the kinematic model of the parallel mechanism.

The protocol is repeated until all the legs in the mechanism are identified.

With respect to traditional identification algorithms for the kinematic identification of parallel mechanism [57, 56] the proposed kinematic identification protocol has the following advantages:

1. Reduction of the kinematic identification computational costs. If a linear least-squares estimation of the kinematic parameters is used to solve the identification problem (Eq. 16), then the correction to be applied to the kinematic parameters ($\Delta\varphi$) can be estimated iteratively as [80]:

$$\Delta\varphi = \left(C^T C\right)^{-1} C^T \Delta\mathbf{Q}. \tag{19}$$

The computational cost of the matrix inversion $(C^T C)^{-1}$ is reduced proportionally to the square of the number of legs of the parallel mechanism, Table 3.6.

2. Improvement of the numerical efficiency of the kinematic identification algorithm by the independent identification of the parameters of each leg.

3. Improvement of the kinematic identification by the design of independent experiments optimized for the identification of each leg.

	Traditional kinematic identification	**Divide and conquer identification**
Regressor	$C^T C(N\ n_{limbs}\ \times\ N\ n_{limbs})$	$C_\kappa^T C_\kappa(N \times N)$
Computational cost (Matrix inversion)	$\propto N^3\ {n_{limbs}}^3$	$\propto N^3\ n_{limbs}$

Table 6: Computational and measurement costs of kinematic identification.

The kinematic identification of parallel mechanisms protocol is applied in the simulated identification of a planar 5R symmetrical mechanism in section 3.7.

3.7 Results

The results on kinematic identification of parallel mechanisms by a Divide and Conquer strategy are presented using a case study: the kinematic identification of the planar 5R symmetrical parallel mechanism.

The planar 5R symmetrical mechanism (Fig. 10) was proposed as a mean to overcome the reduced load-carrying capacity of planar two-degree-of-freedom serial-type manipulators [81]. The mechanism has two degrees-of-freedom (DOF) that allows to positioning the end-effector point (P) in the plane that contains the mechanism. The mechanism is formed by two driving links (l_1 and l_2) and a conducted dyad (L_1 and L_2), Fig. 10. Several research works were developed for the planar 5R symmetrical mechanism. A complete characterization of the assembly configurations [82], kinematic design [81, 77, 83, 84], workspace [81, 82, 77], singularities [81, 82, 77] and

performance atlases [83] are reported. However, no research is reported on kinematic identification. The planar 5R symmetrical mechanism is an instance of the parallel symmetrical mechanisms defined in section 3.5.

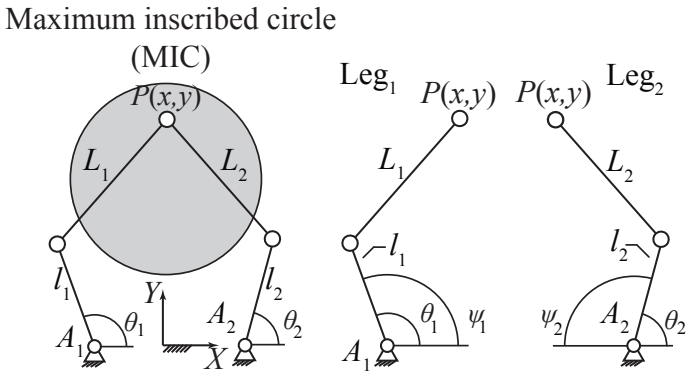

Figure 10: Planar 5R symmetrical mechanism

The kinematic identification of the planar 5R symmetrical mechanism is simulated using the kinematic identification of parallel symmetrical mechanisms protocol (section 3.6) under the following conditions:

1. A linear model is assumed for the active joints A_κ:

$$\theta_\kappa = k\psi_\kappa + \gamma_\kappa, \tag{20}$$

   where the k_κ represent the joint gain, γ_κ is the joint offset, ψ_κ is the measured active joint angle and θ_κ is the active joint angle, $\kappa = 1, 2$.

2. In parallel mechanisms the principal source of error in positioning is due to limited knowledge of the joint centers, leg lengths and active joint parameters [62]. In consequence, the parameters to be estimated are the attachment points (A_κ), the leg lengths ($l_\kappa,\ L_\kappa$), and the joint gain and offset ($k_\kappa,\ \gamma_\kappa$), $\kappa = 1, 2$:

$$\varphi_\kappa = [l_\kappa\ L_\kappa\ A_{\kappa x}\ A_{\kappa y}\ k_\kappa\ \gamma_\kappa]^T. \tag{21}$$

3. The external parameters associated with the measuring device will not be identified. For the external measuring system this implies that its position is known and coincident with the reference frame $X - Y$ and the measurement target is coincident with the end-effector point.

4. The nominal kinematic parameters of the mechanism are disturbed adding a random error with normal distribution and a standard deviation σ. The nominal and disturbed parameters are shown in Table 7.

		Nominal parameters	**Disturbed (real) parameters**
A_{1x}	[m]	-0.5000	-0.4988
A_{1y}	[m]	0.0000	0.0028
k_1		1.0000	1.004
γ_1	[rad]	0.0000	0.0048
l_1	[m]	0.7500	0.7507
L_1	[m]	1.1000	1.0995
A_{2x}	[m]	0.5000	0.4961
A_{2y}	[m]	0.0000	0.0066
l_2	[m]	0.7500	0.7559
L_2	[m]	1.1000	1.0959
k_2		-1.0000	-0.9984
γ_2	[rad]	3.1416	3.1418

Table 7: Identification results.

5. The constrain equation of the inverse kinematics is defined to be, Fig. 11:

$$\mathbf{P} = \mathbf{A} + \mathbf{l} + \mathbf{L}, \tag{22}$$

The Eq. 22 is developed for the κth leg, $\kappa = 1, 2$:

$$L_\kappa{}^2 = (x - l_\kappa \cos\theta_\kappa - A_{\kappa x})^2 + (y - l_\kappa \sin\theta_\kappa - A_{\kappa y})^2. \tag{23}$$

6. The end-effector and joint workspace are limited by the maximal inscribed workspace (MIW), Fig. 10. The MIW corresponds to the maximum singularity-free-end-effector workspace limited by a circle [84].

7. A linearization of the inverse kinematics is used for iteratively solving the non-linear optimization problem (Eq. 16), then, for the jth identification pose the

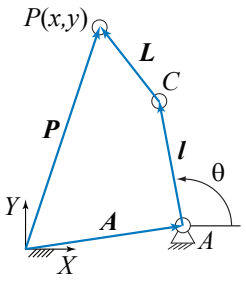

Figure 11: Planar 5R symmetrical mechanism. Leg loop.

identification problem of the κth leg is in the form:

$$\begin{aligned} \Delta \mathbf{q}_\kappa^j = \frac{\partial g_\kappa^j}{\partial \varphi_\kappa} \Delta \varphi_\kappa = C_\kappa^j \Delta \varphi, \\ \Delta \mathbf{q}_\kappa^j = \hat{\mathbf{q}}_\kappa^j - \bar{\mathbf{q}}_\kappa^j, \\ \Delta \varphi_\kappa = \bar{\varphi}_\kappa - \varphi_\kappa. \end{aligned} \tag{24}$$

Using N measurements to identify the set of parameters φ_κ the identification problem is stated in the following manner:

$$\begin{aligned} \Delta \mathbf{Q}_\kappa = C_\kappa \Delta \varphi_\kappa, \\ C_\kappa = \left[C_\kappa^1 \ \cdots C_\kappa^N \right]^T, \\ \Delta \mathbf{Q}_\kappa = \left[\Delta \mathbf{q}_\kappa^1 \cdots \Delta \mathbf{q}_\kappa^N \right]^T, \end{aligned} \tag{25}$$

were C_κ is the total identification matrix of the κth leg. The parameters of the κth leg can be updated using a linear least-squares solution of Eq. 25, [80]:

$$\Delta \varphi_\kappa = (C_\kappa^T C_\kappa)^{-1} C_\kappa^T \Delta \mathbf{Q}_\kappa. \tag{26}$$

8. Each leg is identified using a set of 18 postures of the mechanism to measure the end-effector position and the corresponding active joint variable. The designed sets of identification postures in the end-effector workspace are presented in Fig. 12b (left leg) and Fig. 12c (right leg).

9. The set of end-effector measurements ($\hat{\mathbf{R}}_\kappa$) and its corresponding active joint measurements ($\hat{\mathbf{Q}}_\kappa$) are simulated using forward kinematics and adding random disturbances with normal distribution and standard deviation $\sigma = 1{\cdot}10^{-4}$.

10. An alternative traditional kinematic identification by inverse kinematic modeling is calculated and used as a comparison with respect to the divide and conquer strategy. The traditional identification is performed by means of a set of 36 optimized postures selected in order to maximize the observability of the total identification matrix. The observability was defined as the Eq. 18. The designed set of identification postures is presented in fig. 12a.

The results of the kinematic identification under these conditions are presented in Fig. 12, (selected postures for kinematic identification), Fig. 13 (residual errors in kinematic parameters before and after calibration). The residual errors are calculated as the difference between the real (virtually disturbed) parameters and the estimated parameters. Finally, Fig. 14 presents the estimated local root mean square error for the MIW after calibration. Additionally the computational and measurement identification costs are estimated for the identification of the planar 5R parallel mechanism, Table 8. The measurement costs of the Divide and Conquer strategy are incremented with respect to a traditional identification method 8. The increment of the measurements is required for the independent identification of the legs: each leg requires an independent set of end-effector measurements. In the case of a traditional identification the set of end-effector measurements is common to all the legs. In despite of the measurement increment the Divide and Conquer identification results in a superior estimation with respect to a traditional kinematic identification methods [57, 56].

The conclusions of the paper are proposed in section 3.8.

	Traditional kinematic identification	**Divide and conquer identification**
Regressor	$C^T C(36 \times 36)$	$C_\kappa^T C_\kappa(18 \times 18)$
Computational cost (Matrix inversion)	$\propto 18^3 \cdot 2^3$	$\propto 18^3 \cdot 2$
Measurement cost	$2 \cdot 18 \cdot 2 = 72$	$18 \cdot 2(2+1) = 108$

Table 8: 5R parallel mechanisms. Computational and measurement costs of kinematic identification.

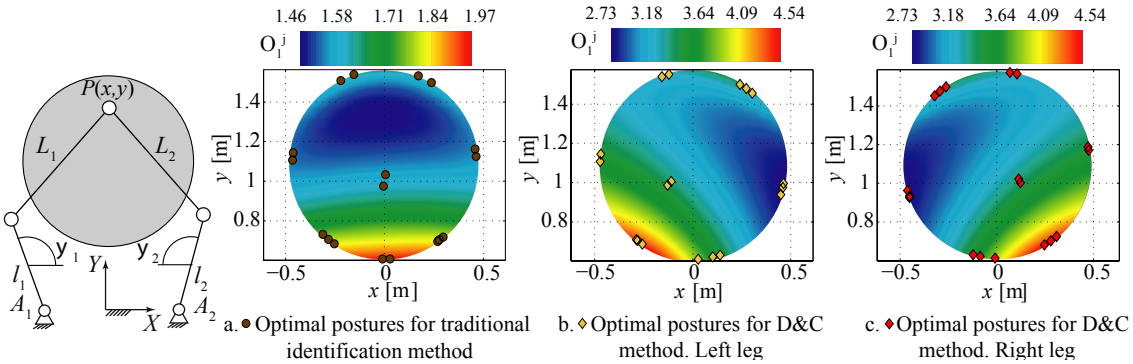

Figure 12: Planar 5R mechanism. Selected postures for kinematic identification.

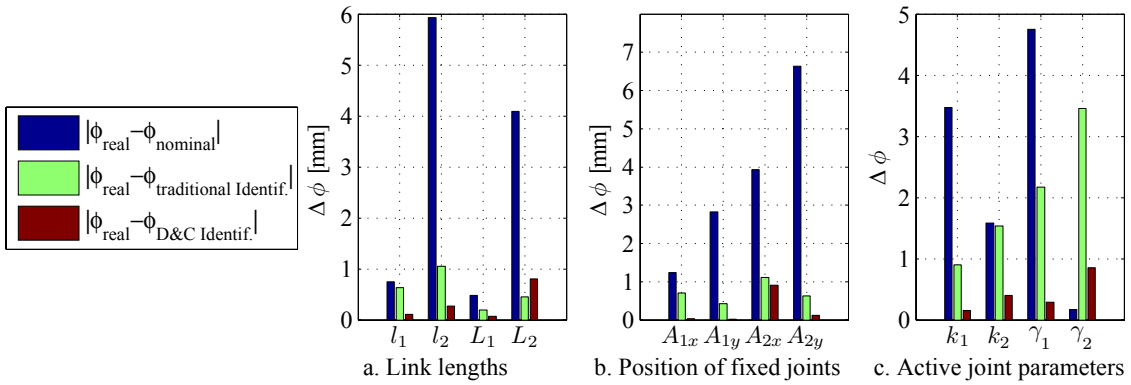

Figure 13: Planar 5R mechanism. Residual errors in the kinematic parameters before and after calibration.

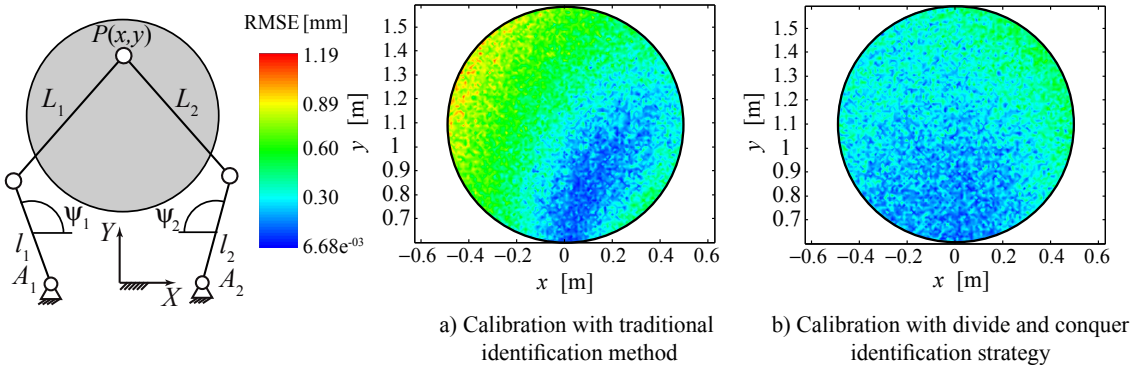

Figure 14: Planar 5R mechanism. Estimated end-effector local root mean square error for the maximal inscribed workspace (MIW) after calibration.

3.8 Conclusions

This article presents a new (Divide and Conquer) strategy for the kinematic identification of parallel symmetrical mechanisms. The new strategy develops a formalization of the inverse calibration method proposed by [56]. The identification strategy (section 3.5) is based on the independent identification of the kinematic parameters of each leg of the parallel mechanism by minimizing an error between the measured active joint variable of the identified leg and their corresponding value, estimated through an inverse kinematic model. With respect to traditional identification methods the Divide and Conquer strategy presents the following advantages:

1. Reduction of the kinematic identification computational costs,
2. Improvement of the numerical efficiency of the kinematic identification algorithm and,
3. Improvement of the kinematic identification results.

Based on the Divide and Conquer strategy, a new protocol for the kinematic identification of parallel symmetrical mechanisms is proposed (section 3.6, Fig. 9). For the selection of optimal identification postures the protocol adopts the active robot calibration algorithm of [78]. The main advantage of the active robot calibration algorithm is the reduction of the complexity of computing an observability index for the kinematic identification, allowing to afford more candidate poses in the optimal pose selection search. The kinematic identification protocol summarizes the advantages of the Divide and Conquer identification strategy and the advantages of the active robot calibration algorithm.

The kinematic identification protocol is demonstrated with the (virtual) identification of a planar 5R symmetrical mechanism (section 3.7). The performance of our identification protocol is compared with a traditional identification method obtaining an improvement of the identification results (Figs. 13 and 14).

4 CONCLUSIONS

This document presents compilation of strategies developed for the prediction of quasi-static deformations in mechanisms considering specially two types of deformations: (1) Intentional and (2) Non-intentional.

For prediction of intentional quasi-static deformations, a computer-based metamodeling methodology for force-displacement modeling of compliant mechanisms using Design of Computer Experiments has been developed. The proposed methodology allows to model compliant mechanisms that have lumped or distributed compliance unlike traditional modeling methods (Pseudo Rigid Body Modeling, Topology Optimization and Numerical Methods). The obtained input-output models using the proposed methodology are enough simple to be used in real-time control. The methodology was applied to obtain a force-displacement model of the six degrees of freedom HexFlex compliant mechanism by finding an accurate model with respect to a FEA simulations.

In the field of prediction of Non-intentional deformations,a new strategy for the kinematic identification of parallel symmetrical mechanisms has been developed. The new identification strategy is based on the independent identification of the kinematic parameters of each leg of the parallel mechanism by minimizing an error between the measured active joint variable of the identified leg and their corresponding value, estimated through an inverse kinematic model. With respect to traditional identification methods this strategy presents the following advantages (1) Reduction of the kinematic identification and computational costs, (2) Improvement of the numerical efficiency of the kinematic identification algorithm and, (3) improvement of the kinematic identification results. This strategy has been added on a new protocol for the kinematic identification of parallel symmetrical mechanisms.

During the development of this work new skills in research, literature reviewing, scientific rhetoric, paper writing and oral presentation have been developed and strengthened. Also it is important to remark that the valuable interaction with advisers, professors, and researchers at EAFIT University was essential in the successful development of this work.

5 REFERENCES

[1] M.L. Culpepper and G. Anderson. Desing of a low-cost nano-manipulator wich utilizes a monolithic, spatial compliant mechanism. *Precision Engineering*, 28:469–482, 2004.

[2] Arthur G. Erdman and George N. Sandor. *Mechanism design (3rd ed.): analysis and synthesis (Vol. 1)*. Prentice-Hall, Inc., Upper Saddle River, NJ, USA, 1997.

[3] J.W. Ryu, S.Q. Lee, D.G. Gweon, and K.S. Moon. Inverse kinematic modeling of a coupled flexure hinge mechanism. *Mechatronics*, 9(6):657–674, 1999.

[4] J. il Jeong, D. Kang, Y.M. Cho, and J. Kim. Kinematic calibration for redundantly actuated parallel mechanisms. *Journal of Mechanical Design*, 126:307, 2004.

[5] Arthur G. Erdman and George N. Sandor. *Advanced mechanism design: analysis and synthesis (Vol. 2)*. Prentice-Hall, Inc., Upper Saddle River, NJ, USA, 1984.

[6] A. Nahvi, J.M. Hollerbach, and V. Hayward. Calibration of a parallel robot using multiple kinematic closed loops. In *IEEE International conference on robotics and automation*, pages 407–407. Citeseer, 1994.

[7] Z Luo, L Tong, M Wang, and S Wang. Shape and topology optimization of compliant mechanisms using a parameterization level set method. *Journal of Computational Physics*, 227(1):680–705, Nov 2007.

[8] Brian D. Jensen and Larry L. Howell. The modeling of cross-axis flexural pivots. *Mechanism and Machine Theory*, 37(5):461–476, 2002.

[9] L.L. Howell. *Compliant mechanisms*. Wiley-Interscience, 2001.

[10] G.K. Ananthasureh and Sridhar Kota. Designing compliant mechanisms. *Mechanical Engineering*, 117(11):93–96, 1995.

[11] S. Venanzi, P. Giesen, and V. Parenti-Castelli. A novel technique for position analysis of planar compliant mechanisms. *Mechanism and Machine Theory*, 40:1224–1239, 2005.

[12] M.H.F. Dado. Limit position synthesis and analysis of compliant 4-bar mechanisms with specified energy levels using variable parametric pseudo-rigid-body model. *Mechanism and Machine Theory*, 40:977–992, 2005.

[13] Zhenyu Liu and J.G. Korvink. Using artificial reaction force to design compliant mechanism with multiple equality displacement constrains. *Finite Element in Analysis and Design*, 45:555–568, 2009.

[14] Kerr-Jia Lu and Sridhar Kota. Parameterization strategy for optimization of shape morphing compliant mechanisms using load path representation. In *Proceedings of DETC03*. ASME, 2003.

[15] Gang-Won Jang, Kyung Joo Kim, and Yoon Young Kim. Integrated topology and shape optimization software for compliant mems mechanism design. *Advances In Engineering Software*, 39:1–14, 2008.

[16] P. Bernardoni, P. Bidaud, C. Bidard, and F. Gosselin. A new compliant mechanism design methodology based on flexible building blocks. *Smart Material and Structures, USA*, 5383:244–254, 2004.

[17] T.W. Simpson, J.D. Peplinski, P.N. Koch, and J.K.Allen. Metamodels for computer-based engineering desing: survey and recommendations. *Engineering with computers*, 17:129–150, 2001.

[18] S.B. Crary. Design of computer experiments for metamodel generation. *Analog Integrated Circuits and Signal Processing*, 32:7–16, 2002.

[19] M.L. Culpepper, G. Anderson, and P. Petri. Hexflex: A planar mechanism for six-axis manipulation and aligment. In *ASPE Annual Meeting*. ASPE, 2002.

[20] M.L. Culpepper. Multiple degree of freedom compliant mechanism. United States Patent, Number: US007270319B, September 2007.

[21] I. Her and JC Chang. A linear scheme for the displacement analysis of micropositioning stages with flexure hinges. *Journal of Mechanical Design*, 116:770, 1994.

[22] B.P. Trease, Y.M. Moon, and S. Kota. Design of large-displacement compliant joints. *Journal of Mechanical Design*, 127:788, 2005.

[23] C.M. Dibiaso. Comparison of molecular simulation and pseudo-rigid-body model predictions for a carbon nanotube based compliant parallel-guiding mechanism. *Journal of Mechanical Design*, 130(04):2302–1–8, 2008.

[24] W.K. Kim, D.G. Kim, and B.J. Yi. Analysis of a planar 3 degree-of-freedom adjustable compliance mechanism. *Journal of Mechanical Science and Technology*, 10(3):286–295, 1996.

[25] P.G. Opdahl, B.D. Jensen, and L.L. Howell. An investigation into compliant bistable mechanisms. In *Proc. 1998 ASME Design Engineering Technical Conf*, 1998.

[26] S.L. Chang, J.J. Lee, and H.C. Yen. Kinematic and compliance analysis for tendon-driven robotic mechanisms with flexible tendons. *Mechanism and machine theory*, 40(6):728–739, 2005.

[27] Y.K. Yong and T.F. Lu. Kinetostatic modeling of 3-RRR compliant micromotion stages with flexure hinges. *Mechanism and Machine Theory*, 44(6):1156–1175, 2009.

[28] N. Lobontiu, J.S.N. Paine, E. Garcia, and M. Goldfarb. Design of symmetric conic-section flexure hinges based on closed-form compliance equations. *Mechanism and machine theory*, 37(5):477–498, 2002.

[29] RW Brockett and A. Stokes. On the synthesis of compliant mechanisms. In *1991 IEEE International Conference on Robotics and Automation, 1991. Proceedings.*, pages 2168–2173, 1991.

[30] N. Lobontiu, J.S.N. Paine, E. Garcia, and M. Goldfarb. Corner-filleted flexure hinges. *Journal of Mechanical Design*, 123:346, 2001.

[31] A. Saxena and SN Kramer. A simple and accurate method for determining large deflections in compliant mechanisms subjected to end forces and moments. *Journal of Mechanical Design*, 120:392, 1998.

[32] SR Park and SH Yang. A mathematical approach for analyzing ultra precision positioning system with compliant mechanism. *Journal of Materials Processing Tech.*, 164:1584–1589, 2005.

[33] A. Banerjee, B. Bhattacharya, and AK Mallik. Forward and inverse analyses of smart compliant mechanisms for path generation. *Mechanism and Machine Theory*, 44(2):369–381, 2009.

[34] C. Boyle, L.L. Howell, S.P. Magleby, and M.S. Evans. Dynamic modeling of compliant constant-force compression mechanisms. *Mechanism and machine theory*, 38(12):1469–1487, 2003.

[35] T.E. Bruns and D.A. Tortorelli. Topology optimization of non-linear elastic structures and compliant mechanisms. *Computer Methods in Applied Mechanics and Engineering*, 190(26-27):3443–3459, 2001.

[36] A. Saxena. A material-mask overlay strategy for continuum topology optimization of compliant mechanisms using honeycomb discretization. *Journal of Mechanical Design*, 130(06):2304–1–9, 2008.

[37] M.P. Bendsøe and O. Sigmund. Material interpolation schemes in topology optimization. *Archive of Applied Mechanics (Ingenieur Archiv)*, 69(9):635–654, 1999.

[38] M.P. Bendøse and O. Sigmund. *Topology Optimization: Theory, Methods and Applications*. ISBN: 3-540-42992-1. Springer, 2003, 2003.

[39] CBW Pedersen, NA Fleck, and GK Ananthasuresh. Design of a Compliant Mechanism to Modify an Actuator Characteristic to Deliver a Constant Output Force. *Journal of Mechanical Design*, 128:1101, 2006.

[40] B. Zettl, W. Szyszkowski, and W.J. Zhang. Accurate low dof modeling of a planar compliant mechanism with flexure hinges: the equivalent beam methodology. *Precision Engineering*, 29(2):237 – 245, 2005.

[41] F. De Bona and M.G. Munteanu. Optimized Flexural Hinges for Compliant Micromechanisms. *Analog Integrated Circuits and Signal Processing*, 44(2):163–174, 2005.

[42] A. Saxena and GK Ananthasuresh. Topology synthesis of compliant mechanisms for nonlinear force-deflection and curved path specifications. *Journal of Mechanical Design*, 123:33, 2001.

[43] M. Callegari, A. Cammarata, A. Gabrielli, M. Ruggiu, and R. Sinatra. Analysis and Design of a Spherical Micromechanism With Flexure Hinges. *Journal of Mechanical Design*, 131:051003, 2009.

[44] S. Zhang and E.D. Fasse. A finite-element-based method to determine the spatial stiffness properties of a notch hinge. *Journal of Mechanical Design*, 123:141, 2001.

[45] H. Zhou and K.L. Ting. Geometric Optimization of Spatial Compliant Mechanisms Using Three-Dimensional Wide Curves. *Journal of Mechanical Design*, 131:051002, 2009.

[46] Kai-Tai and Runze Li. Uniform design for computer experiments and its optimal properties. *International Journal of Materials and Product Technology*, 25:2058–2080, 2006.

[47] R.P. Paul. *Robot manipulators: mathematics, programming, and control*. MIT Press Cambridge, MA, USA, 1982.

[48] G.E.P. Box, W.G. Hunter, and J.S Hunter. *Use of Data Sampling, Surrogate Models, and Numerical Optimization in Engineering Design*. Jhon Wiley and Sons, New York, 1978.

[49] NIST. Engineering statistics handbook.nist/sematech e-handbook of statistical methods, November 2008.

[50] R.V. Lenth. Quick and easy analysis of unreplicated factorials. *Technometrics*, 31(4):469–473, 1989.

[51] K.T. Fang, D.K.J Lin, P. Winker, and Y. Zhang. Uniform design: theory and application. *Technometrics*, 42(3):237–248, 2000.

[52] T.W. Simpson, J.D. Peplinski, P.N. Koch, and J.K.Allen. On the use of statistics in design and the implications for deterministic computer experiments. In *1997 ASME Design Engineering Technical Conferences*, 1997.

[53] D.M. Bates and S. DebRoy. Linear mixed models and penalized least squares. *Journal of Multivariate Analysis*, 91(1):1–17, 2004.

[54] D. Ruppert and M.P. Wand. Multivariate locally weighted least squares regression. *The annals of statistics*, pages 1346–1370, 1994.

[55] P.A. Petri. *A continuum mechanic design aid for non-planar compliant mechanisms*. PhD thesis, Massachusetts Institute of Technology, 2002.

[56] H. Zhuang, J. Yan, and O. Masory. Calibration of Stewart platforms and other parallel manipulators by minimizing inverse kinematic residuals. *Journal of Robotic Systems*, 15(7), 1998.

[57] P. Renaud, A. Vivas, N. Andreff, P. Poignet, P. Martinet, F. Pierrot, and O. Company. Kinematic and dynamic identification of parallel mechanisms. *Control Engineering Practice*, 14(9):1099–1109, 2006.

[58] J.P Merlet. *Parallel Robots*. Springer Netherlands, second edition, 2006.

[59] J. Hollerbach, W. Khalil, and M. Gautier. *Springer Handbook of Robotics, Model Identification*. Springer, 2008.

[60] L.W. Tsai. *Robot analysis: the mechanics of serial and parallel manipulators*. Wiley-Interscience, 1999.

[61] S. Besnard and W. Khalil. Identifiable parameters for parallel robots kinematic calibration. In *IEEE International Conference on Robotics and Automation, 2001. Proceedings 2001 ICRA*, volume 3, 2001.

[62] D. Daney, I. Lorraine, and V.L.N. LORIA. Optimal measurement configurations for Gough platform calibration. In *IEEE International Conference on Robotics and Automation, 2002. Proceedings. ICRA'02*, volume 1, 2002.

[63] D. Daney, Y. Papegay, and B. Madeline. Choosing measurement poses for robot calibration with the local convergence method and Tabu search. *The International Journal of Robotics Research*, 24(6):501, 2005.

[64] C.C. Iuraşcu and F.C.P. Park. Geometric algorithms for kinematic calibration of robots containing closed loops. *Journal of Mechanical Design*, 125:23, 2003.

[65] Y. Koseki, T. Arai, K. Sugimoto, T. Takatuji, and M. Goto. Design and accuracy evaluation of high-speed and high precision parallel mechanism. In *IEEE International Conference on Robotics and Automation (ICRA)*, volume 3, pages 1340–1345. Citeseer, 1998.

[66] H. Zhuang, O. Masory, and J. Yan. Kinematic calibration of a Stewart platform using pose measurements obtained by a single theodolite. In *1995 IEEE/RSJ International Conference on Intelligent Robots and Systems 95.'Human Robot Interaction and Cooperative Robots', Proceedings*, volume 2, 1995.

[67] T. Huang, D.G. Chetwynd, D.J. Whitehouse, and J. Wang. A general and novel approach for parameter identification of 6-dof parallel kinematic machines. *Mechanism and machine theory*, 40(2):219–239, 2005.

[68] H. Chanal, E. Duc, P. Ray, and JY. Hascoet. A new approach for the geometrical calibration of parallel kinematics machines tools based on the machining of a dedicated part. *International Journal of Machine Tools and Manufacture*, 47(7-8):1151–1163, 2007.

[69] H. Wang and K.C. Fan. Identification of strut and assembly errors of a 3-PRS serial–parallel machine tool. *International Journal of Machine Tools and Manufacture*, 44(11):1171–1178, 2004.

[70] A. Pashkevich, D. Chablat, and P. Wenger. Kinematic calibration of Orthoglide-type mechanisms from observation of parallel leg motions. *Mechatronics*, 19(4):478–488, 2009.

[71] Deuk Soo Kang, Tae Won Seo, and Jongwon Kim. Development and kinematic calibration for measurement structure of a micro parallel mechanism platform. *Journal of Mechanical Science and Technology*, 22:746–754, 2008.

[72] P. Last and J. Hesselbach. A new calibration strategy for a class of parallel mechanisms. *Advances in Robot Kinematics: Mechanisms and Motion*, pages 331–338, 2006.

[73] In-Chul Ha. Kinematic parameter calibration method for industrial robot manipulator using the relative position. *Journal of Mechanical Science and Technology*, 22(6):1084–1090, 2008.

[74] D. Daney, I.Z. Emiris, Y. Papegay, E. Tsigaridas, and J.P. Merlet. Calibration of parallel robots: on the Elimination of Pose–Dependent Parameters. In *Proc. of the first European Conference on Mechanism Science, EuCoMeS*, 2006.

[75] D. Daney, N. Andreff, G. Chabert, and Y. Papegay. Interval method for calibration of parallel robots: Vision-based experiments. *Mechanism and Machine Theory*, 41(8):929–944, 2006.

[76] J. Ryu and A. Rauf. A new method for fully autonomous calibration of parallel manipulators using a constraint link. In *2001 IEEE/ASME International Conference on Advanced Intelligent Mechatronics, 2001. Proceedings*, volume 1, 2001.

[77] X. Liu, J. Wang, and G. Pritschow. Kinematics, singularity and workspace of planar 5r symmetrical parallel mechanisms. *Mechanism and Machine Theory*, 41(2):145 – 169, 2006.

[78] Yu Sun and J.M. Hollerbach. Active robot calibration algorithm. In *Robotics and Automation, 2008. ICRA 2008. IEEE International Conference on*, pages 1276–1281, May 2008.

[79] J.H. Jang, S.H. Kim, and Y.K. Kwak. Calibration of geometric and non-geometric errors of an industrial robot. *Robotica*, 19(03):311–321, 2001.

[80] J Hollerbach and C Wampler. The calibration index and taxonomy for robot kinematic calibration methods. *The International Journal of Robotics Research*, Jan 1996.

[81] J. J. Cervantes-Sánchez, J. C. Hernández-Rodríguez, and J. Angeles. On the kinematic design of the 5r planar, symmetric manipulator. *Mechanism and Machine Theory*, 36(11-12):1301 – 1313, 2001.

[82] J. J. Cervantes-Sánchez, J. C. Hernández-Rodríguez, and J. G. Rendón-Sánchez. On the workspace, assembly configurations and singularity curves of

the rrrrr-type planar manipulator. *Mechanism and Machine Theory*, 35(8):1117 – 1139, 2000.

[83] X. Liu, J. Wang, and G. Pritschow. Performance atlases and optimum design of planar 5r symmetrical parallel mechanisms. *Mechanism and Machine Theory*, 41(2):119 – 144, 2006.

[84] X. Liu, J. Wang, and H. Zheng. Optimum design of the 5r symmetrical parallel manipulator with a surrounded and good-condition workspace. *Robotics and Autonomous Systems*, 54(3):221 – 233, 2006.